National Sun Yat-sen University

國立中山大學

VSB TECHNICAL UNIVERSITY OF OSTRAVA

The 28th International Energy and Environment Conference

Performance analysis of mixed fuels in low and medium-temperature SOFC

Department of Mechanical and Electro-Mechanical Engineering
National Sun Yat-sen University, Kaohsiung, 804201, Taiwan

Presenter: Prof. Jenn-Kun Kuo

Date: 08-10 September 2025

Heart of the Beskid Mountains

Hydrogen and Fuel Cell Laboratory
氫能與燃料電池實驗室

Industry

Kaohsiung is the third most populated city in Taiwan with **2.77 million residents**. The City has transformed from an industrial center with refining and shipbuilding industries to focus on the semiconductor/ photoelectric, digital content, biomedical, cultural creativity, and tourism industries.

- TSMC Corp.
- ASE Corp.
- CHINA STEEL Corp.
- CHINA PETROLEUM Corp.
- CHINA SHIPBUILDING Corp.
- SEMICONDUCTOR Industry
- CHEMICAL Industry
- MEDICAL Industry

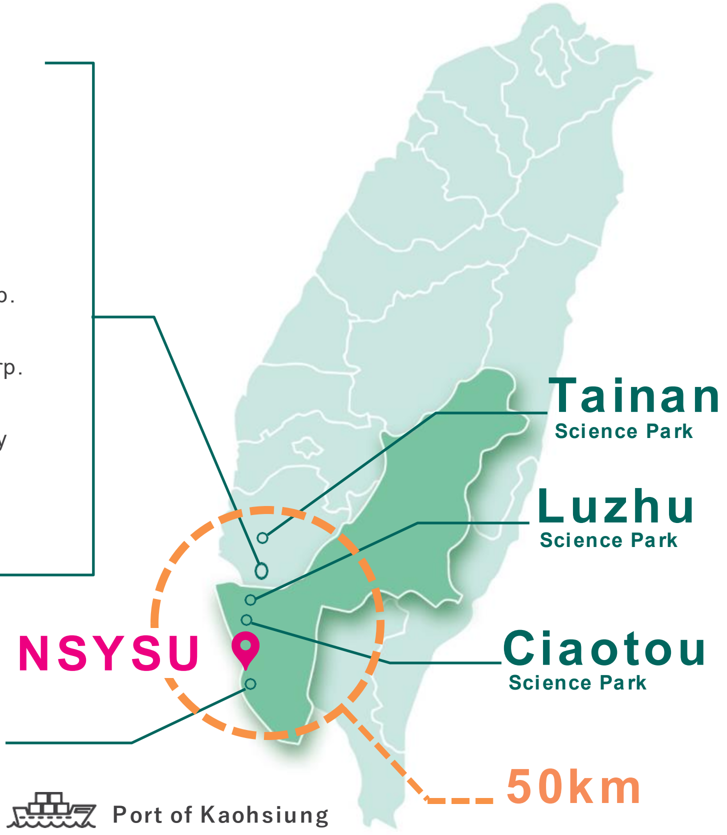

Kaohsiung
Software Technology Park

Kaohsiung City

Climate

Kaohsiung has tropical monsoon climate with an average temperature of 25°C, with high of 35°C in July and low of 10°C in January. Rain and typhoon usually occur in the summer months of June - August.

Metro-rapid transit

Source: Kaohsiung City Government

Transportation

Kaohsiung is easily accessible by the **international airport (KHH)**, **high speed rail (THSR)**, TRA train, metro-rapid transit (KMRT), light rail (LRT), and Kaohsiung i-bus.

Light Tail (LRT)

Source: Kaohsiung City Government

Green Hydrogen Market Expected to Experience Robust Growth with a Projected CAGR(Compound Annual Growth Rate) of 62% during the Forecast Period

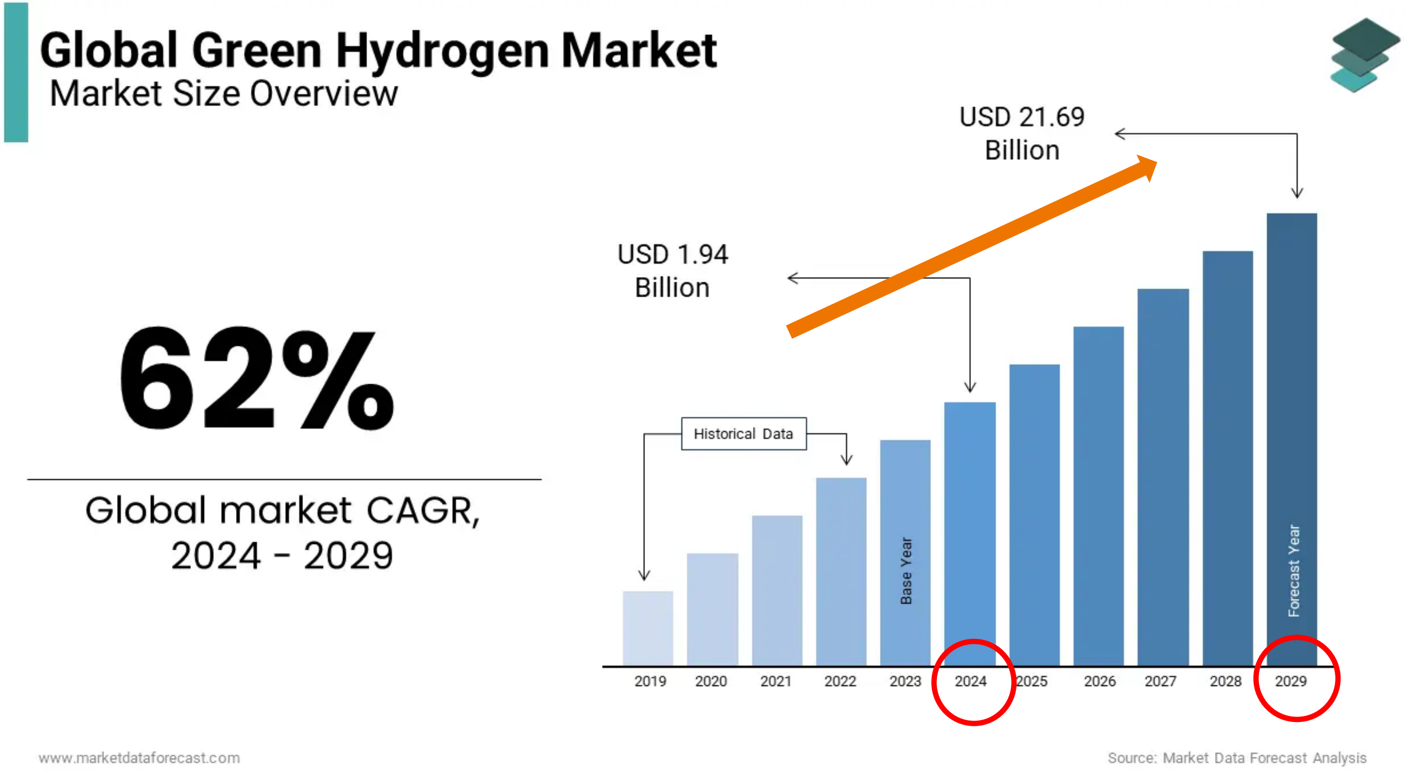

USD 21.69 Billion by 2029 from **USD 1.94 Billion** in 2024

The Green Hydrogen Market's expansion is primarily fueled by government initiatives promoting green hydrogen and renewable energy, driven by growing concern over environmental degradation.

Sources: https://www.globenewswire.com/news

2030 in the Net Zero Emission

Low-emission **hydrogen** is essential for decarbonizing **heavy industry**, **long-distance transport**, and **steelmaking**.

- For highly energy-intensive **transport** (**aviation** and **shipping**).
- In road transport, **hydrogen fuel cell electric vehicles (FCEVs)** more efficient than EV.
- New applications in industry are critical in **steelmaking**.

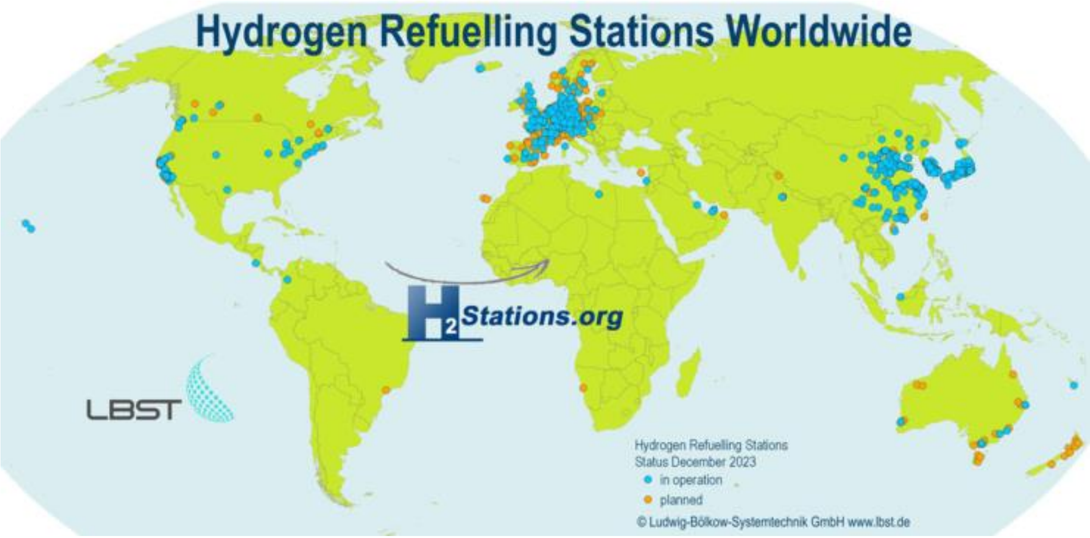

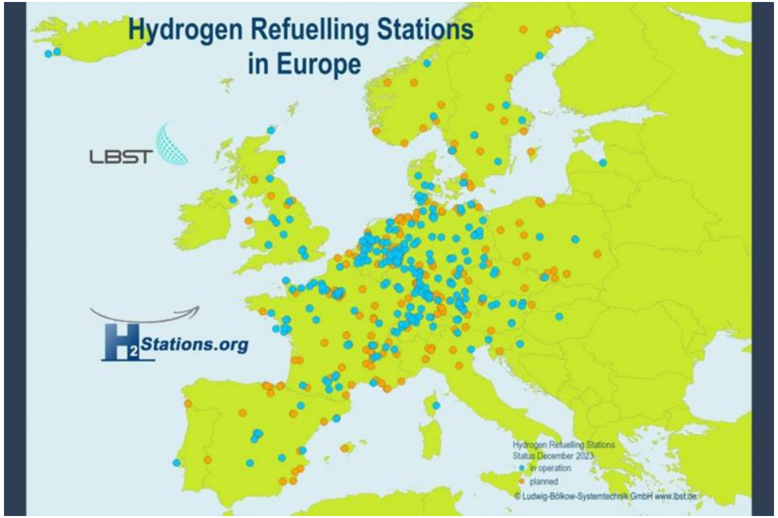

Infrastructure for hydrogen use in transport is expanding-more than over **1160 hydrogen refueling stations** in operation at the mid-2025.

- ✓ **Czech Republic: 4**
- ✓ **Euro: 186**
- ✓ **Japan: 181**
- ✓ **China: 540**
- ✓ **Korea: 198**
- ✓ **Germany: 113**
- ✓ **United States: 89**
- ✓ **Taiwan: 1**

Grey hydrogen, how hydrogen is currently made

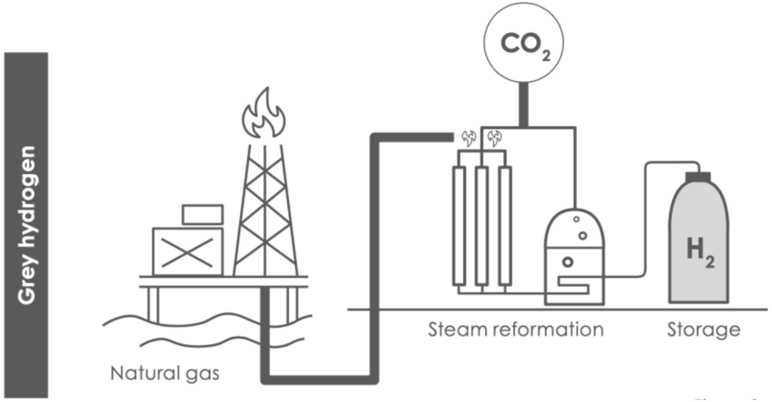

Blue hydrogen, as advocated by the gas supply industry

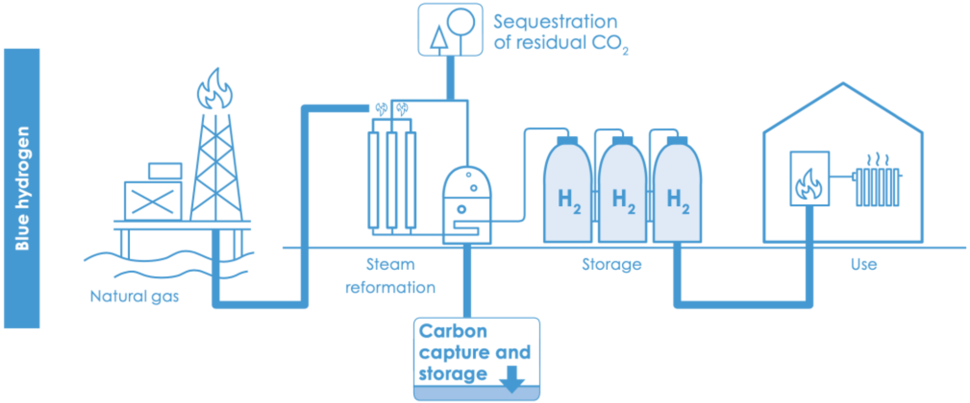

Green hydrogen, made from renewable energy

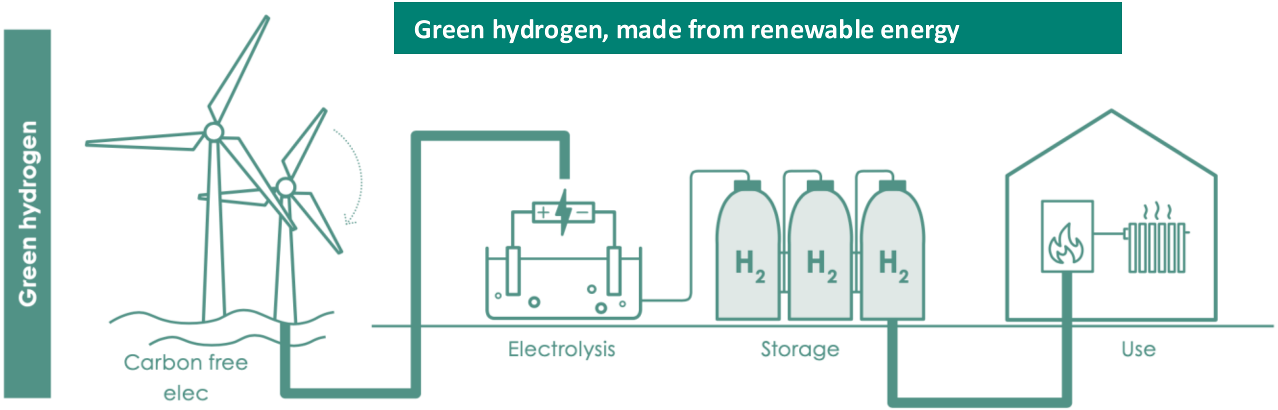

Source: https://h2sciencecoalition.com/briefings/clean-hydrogen-definition/

Blue H_2 Production Emission

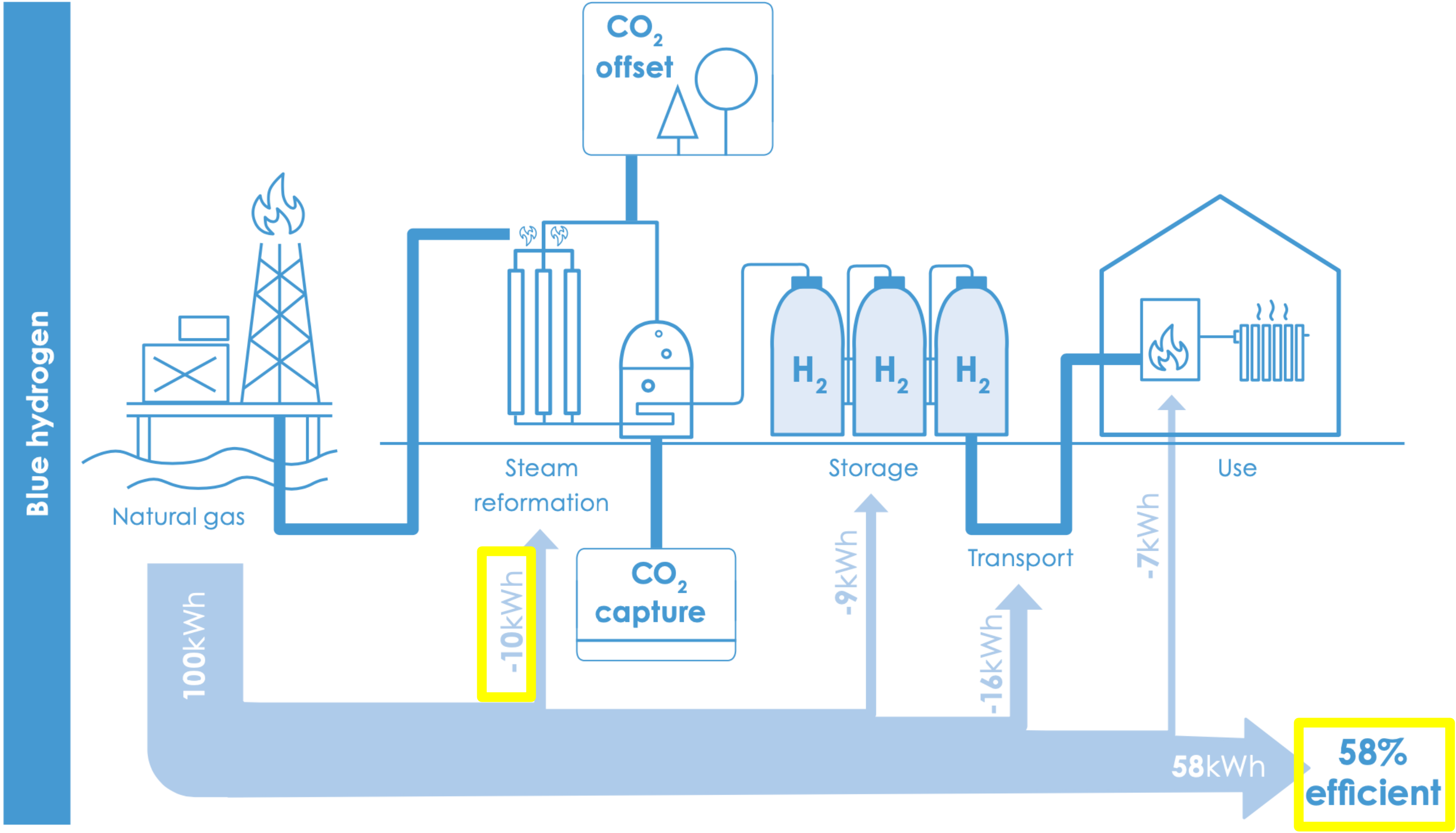

Source: https://h2sciencecoalition.com/briefings/clean-hydrogen-definition/

Green H_2 Production Emission

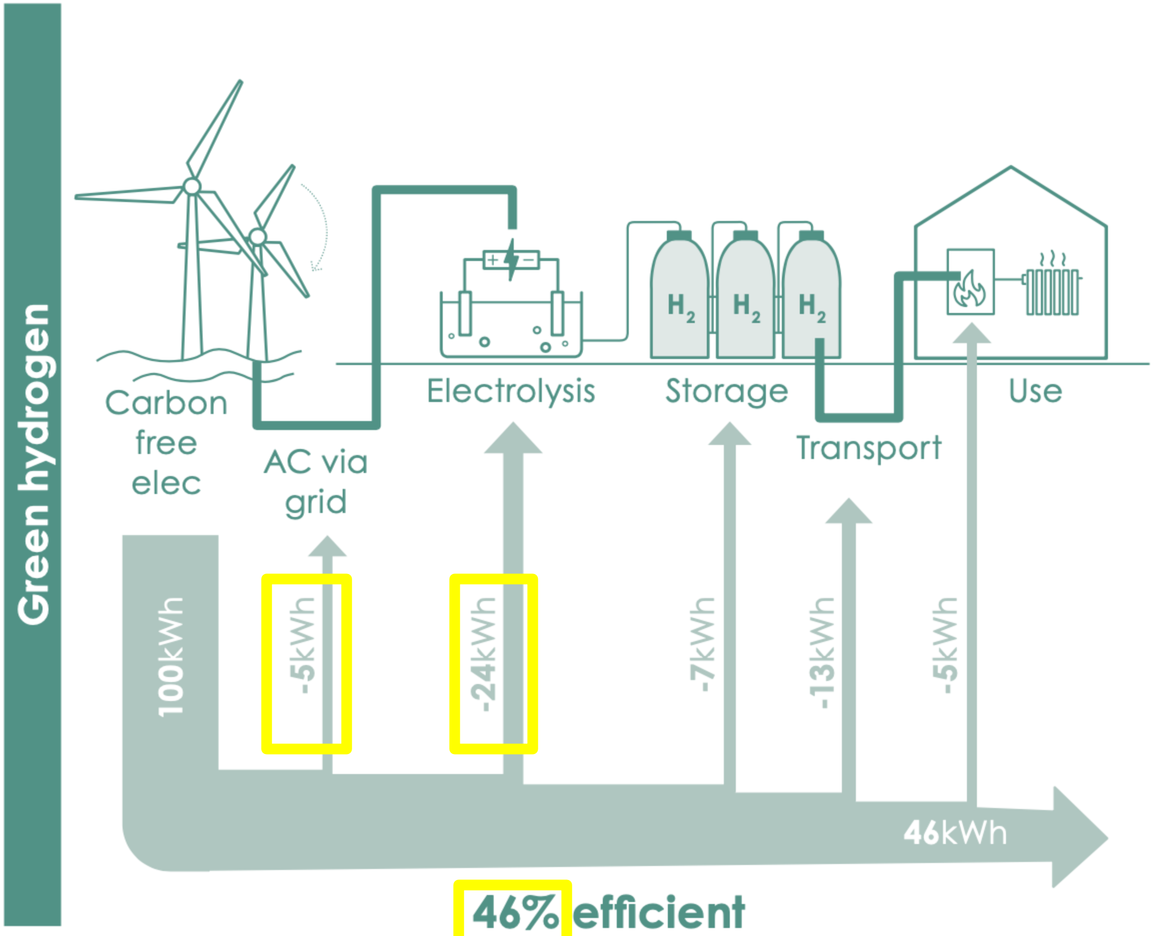

Hydrogen as an **energy delivery carrier** is relatively inefficient compared with using renewable electricity with heat pumps

Hydrogen could provide useful renewable energy storage until needed for winter peaks.

However, this can be more efficiently implemented using re-purposed combined cycle gas turbine (CCGT) power stations without needing more comprehensive gas grid conversion.

Source: https://h2sciencecoalition.com/briefings/clean-hydrogen-definition/

BP plans UK's largest blue and green hydrogen 1 GW project in the Tees Valley in 2017

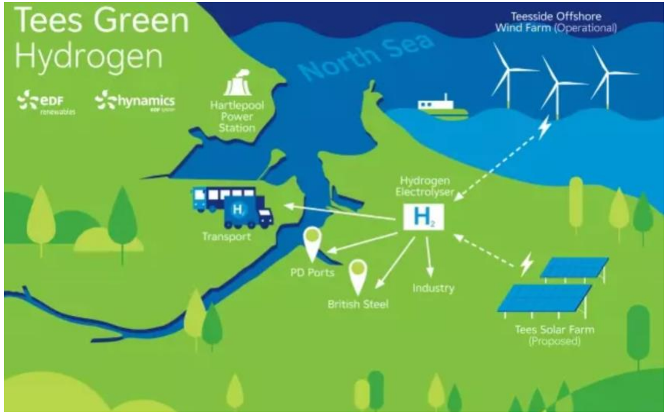

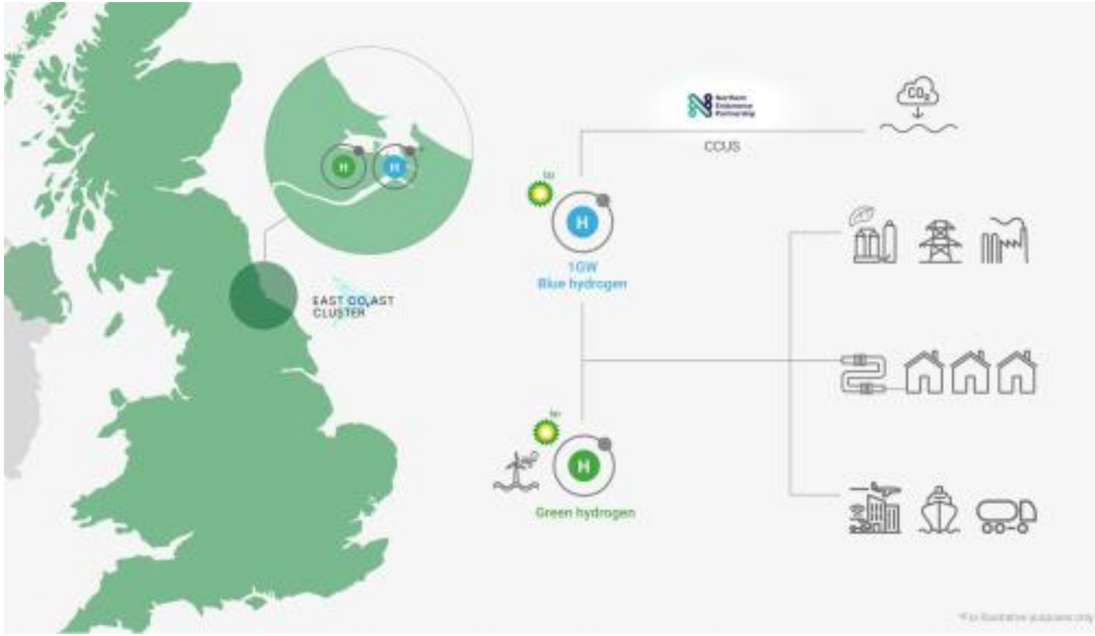

Sources: https://www.offshore-energy.biz/rwe-teams-up-with-kellas-midstream-for-green-hydrogen-production/

World largest hydrogen fuel cell power plant was built in Korea by KOSPO – 135 MW (2025)

- It is in operation in 2021.
- Capable of providing electricity to some 250,000 households.
- The project cost about $300 million.
- It emits little SOX and NOX.
- It can purify fine dust emitted from a nearby liquefied natural gas (LNG) thermal power plant run by KOSPO.
- It would also produce hot water for heating that can be used by about 44,000 households.

SOFC power plant

Hydrogen production cost from the hybrid solar cell and wind power in 2030.

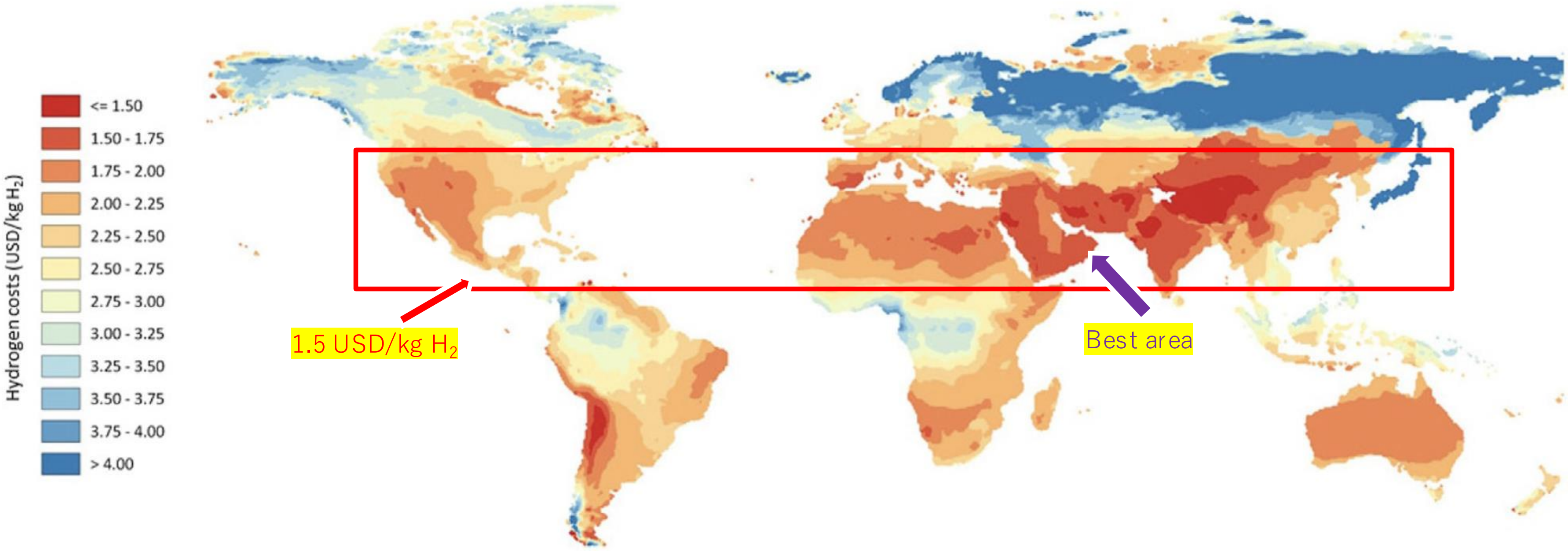

- ✓ This area is very suitable for solar green energy generation.
- ✓ 1.5 USD/kg H_2 that would place it as one of the **cheapest green hydrogen producer** in the world.

Source: https://www.researchgate.net/publication/361926388

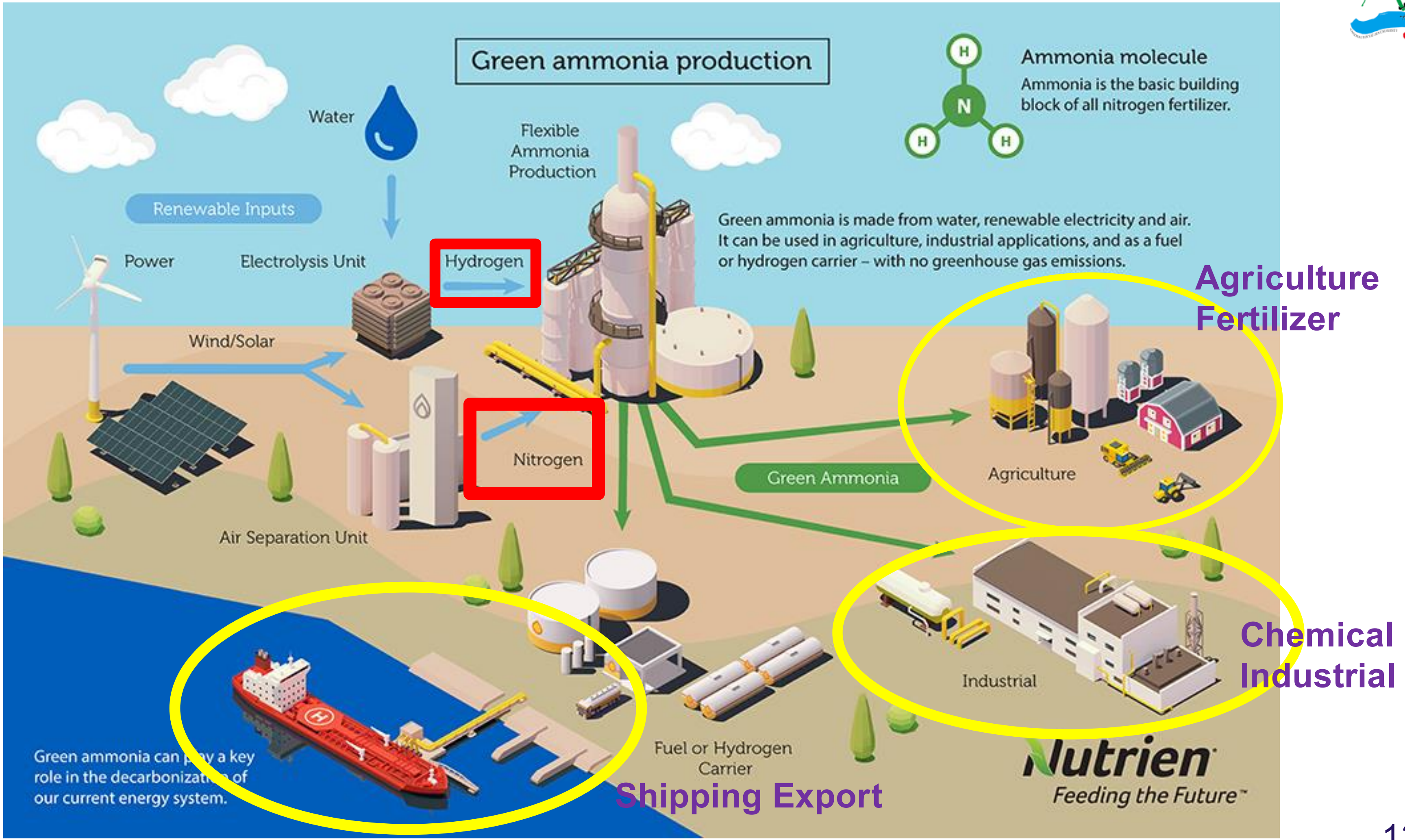

Sources: https://www.nutrien.com/what-we-do/stories/collaboration-key-our-blue-and-green-ammonia-journey

Blue Hydrogen Risks and Dependencies

- **Dependence on CCS technology**
  - A cost-effective scaling up of CCS technology and capacity is essential.

- **Dependence on fossil fuel supply**
  - International market fluctuations will directly impact the cost of production.

- **Emissions from the production**
  - Mainly methane.

Blue Hydrogen Risks and Dependencies

- **Dependence on renewable electricity generation and supply**
  - Significant expansion of renewable energy capacity.

- **Competition for renewable energy between direct electrification and green hydrogen production**

- **Electrolyser build rates and supply of the critical raw materials required**
  - Rising global demand could cause price fluctuations and potentially lead to geopolitical issues.

- **Access to sufficient water supply and sufficient waste management systems, together with the availability and access to renewable electricity**
  - Are crucial factors in determining green production's location and environmental impact.

The various components can be combined in the hydrogen transmission and distribution value chain, leading to specific cost benefits.

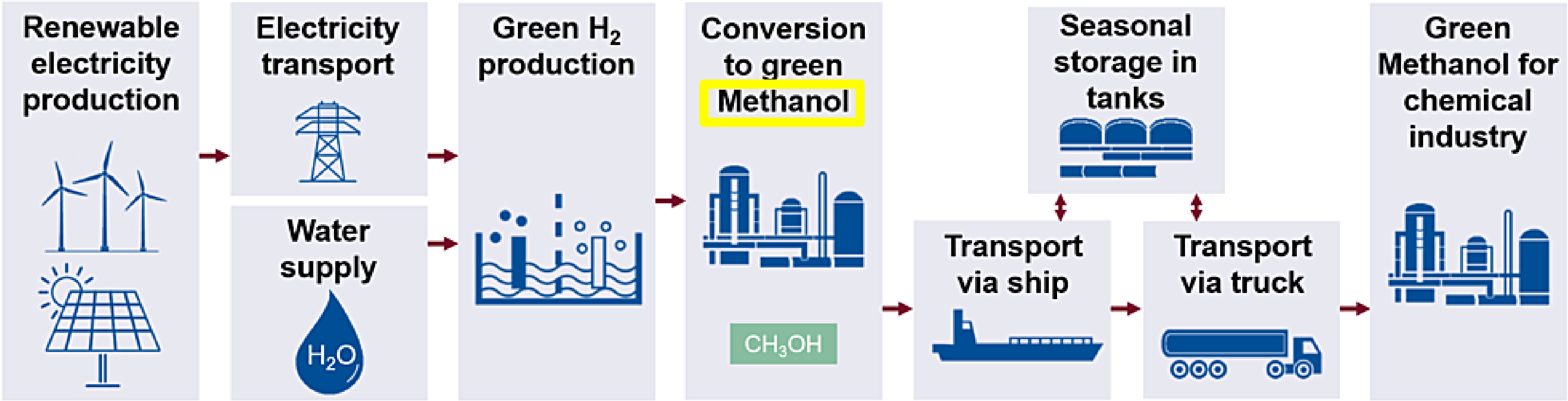

Green methanol production for chemical industry

Safe, Reliable, and Informed Innovation Across the Hydrogen Value Chain

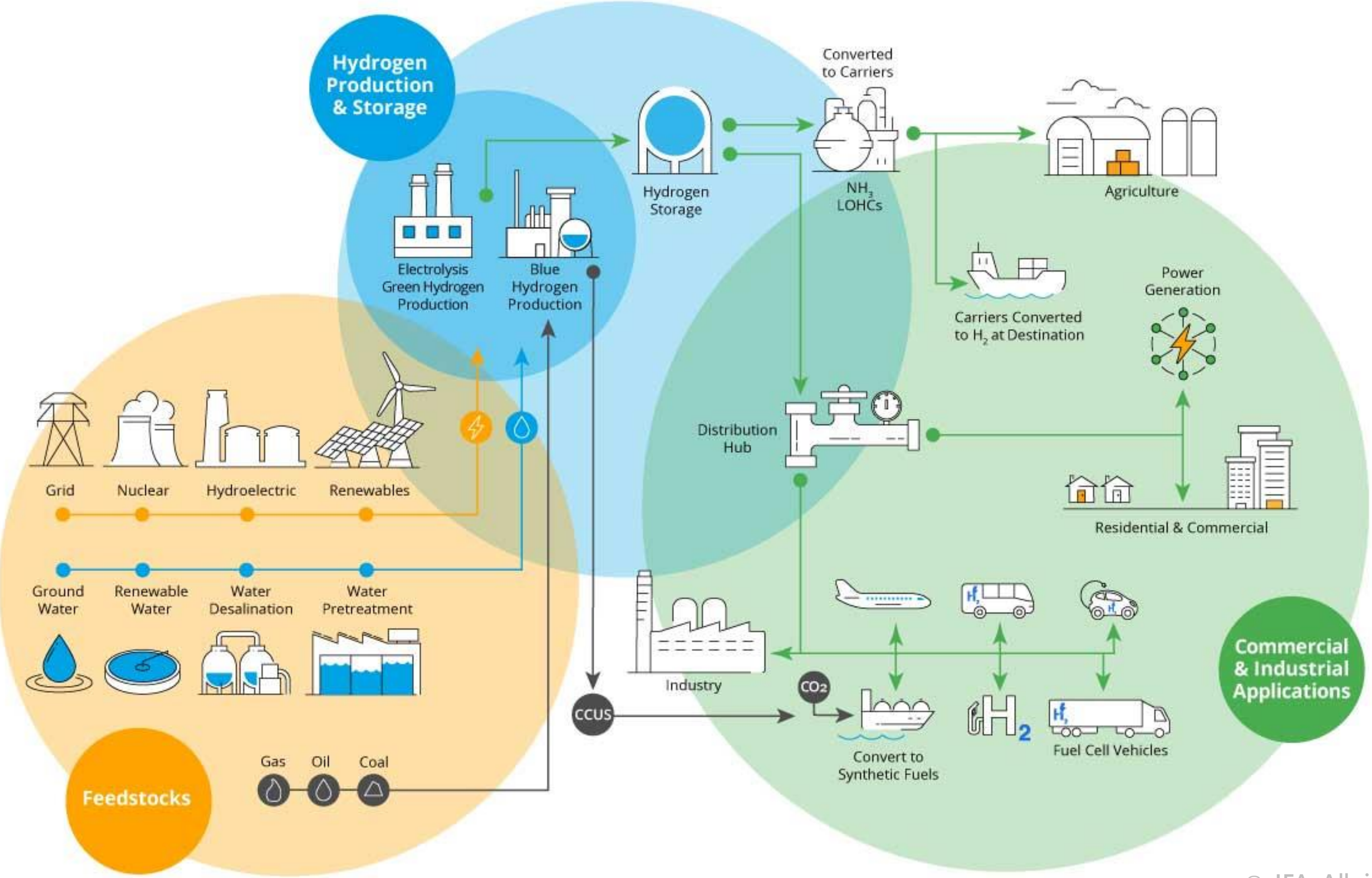

Hydrogen storage

Today hydrogen is most commonly stored as a gas or liquid in tanks for small-scale mobile and stationary applications.

- **Geological storage**

  - The best option for large-scale and long-term storage.

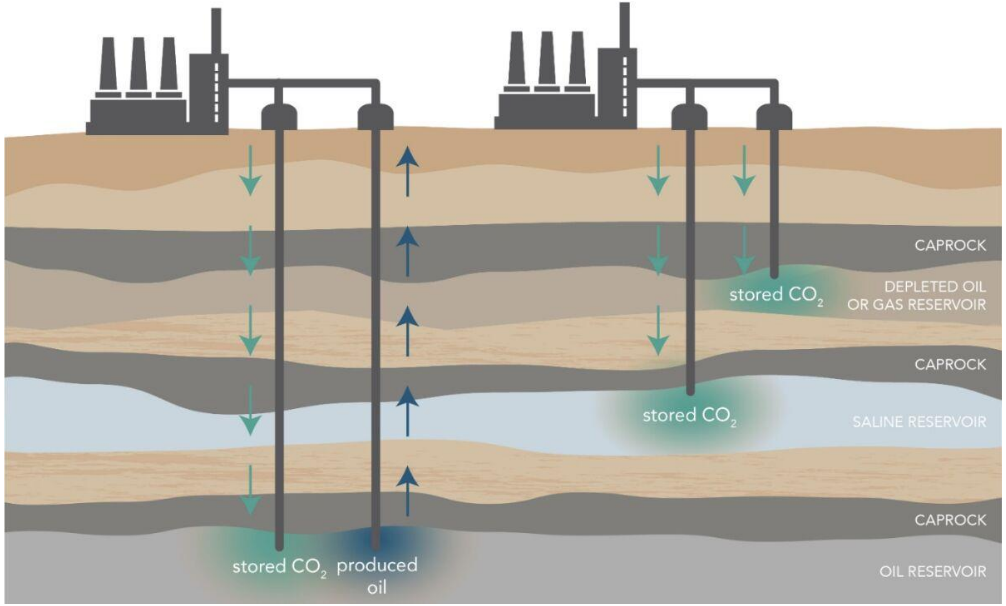

- **Storage tanks**

  - The more suitable for short-term and small-scale storage.

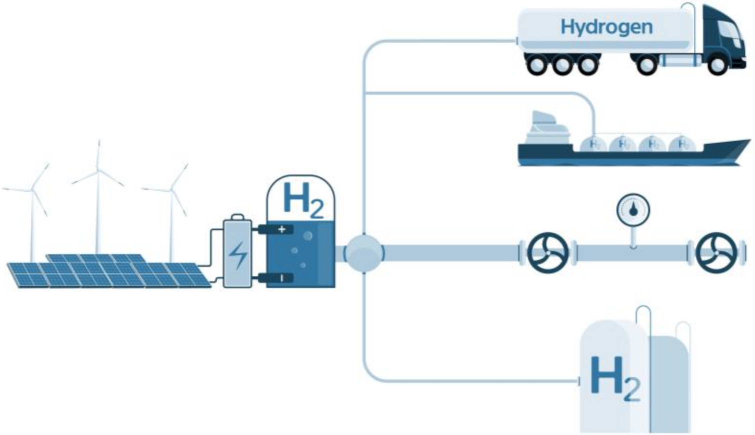

Hydrogen Transmission and Distribution

- The low energy density of hydrogen means that it can be very expensive to transport over long distances.

- Natural gas, pure hydrogen, can be liquefied **before** being transported to increase density.

- Incorporate the hydrogen into large molecules that can be more readily transported as liquids.

- IEA analysis indicates that hydrogen transmission as a gas by pipeline is generally the cheapest option if the hydrogen needs are transported for more than 1500 km.

Hydrogen Transmission and Distribution

- Transporting energy over long distances is easier when the energy is a chemical fuel rather than electricity.
- Pipelines
  - It can be used for a long time (40-80 years).
  - Their two main drawbacks are
    a. the high capital costs entailed.
    b. the need to acquire the right of way by necessity (Country to Country).

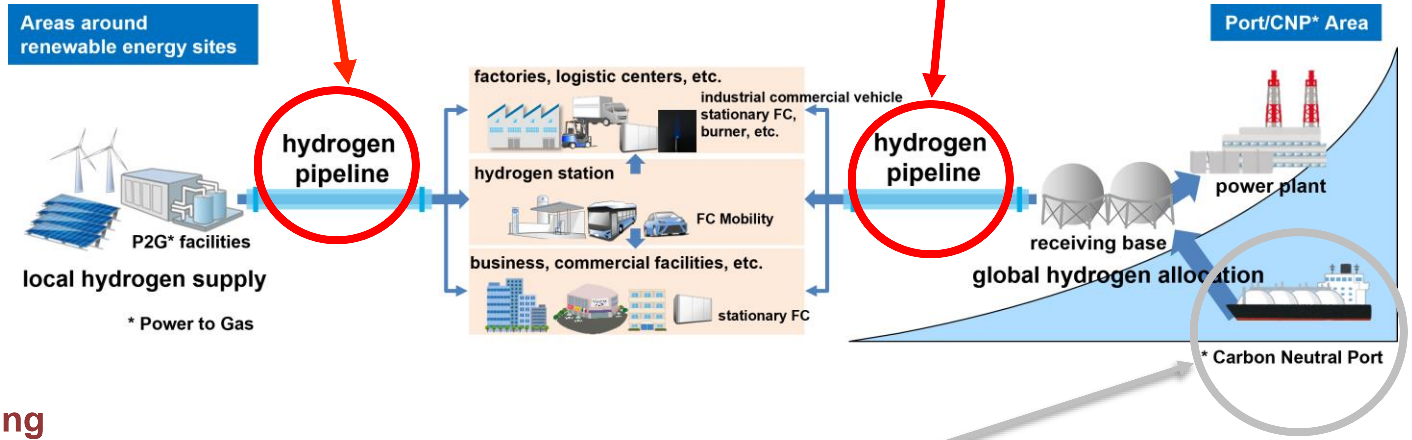

- Shipping
  - Imported hydrogen offers scope for countries to diversify their energy imports, and one result of this is significant interest in using ships to transport hydrogen.

Potential Roles of Hydrogen in Future Energy Systems

- ✓ Industry
- ✓ Transport
- ✓ Heat and Building

Industry

- **Chemical industrial processes**
  - The **hydrogen** demand for **methanol production** will likely **increase** from plastic production shifts away from fossil fuel-based production processes.

- **Primary steelmaking**
  - Hydrogen can substitute fuels as the **sole reducing agent** to produce direct reduced iron and water instead of CO_2 as a by-product.

- **Industrial heating**
  - Hydrogen is likely to be the **only** option available to substitute fossil fuel in certain industrial direct-firing processes (such as furnaces and kilns).

Transport

- **Heavy goods vehicles and public service vehicles**
  - Hydrogen fuel cell electric vehicles.

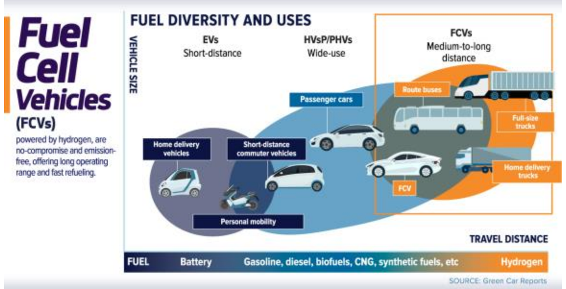

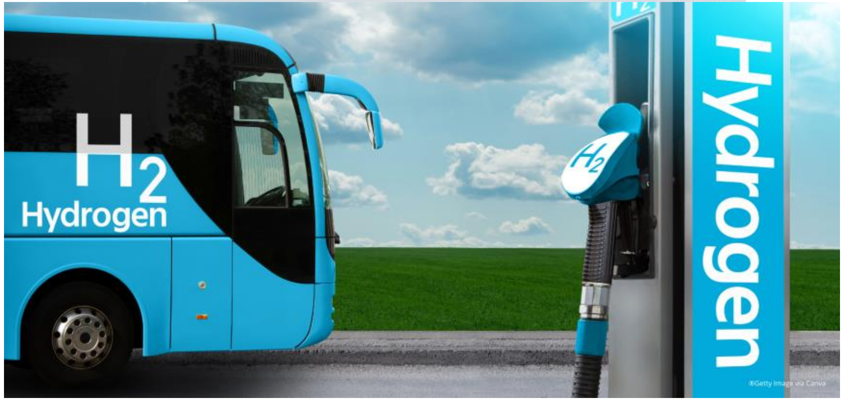

BMW to launch production hydrogen X5 with fuel-cell tech in 2028

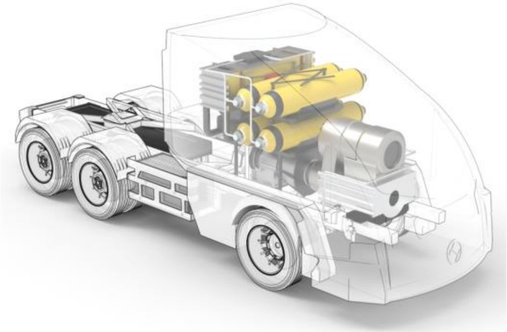

Source: https://www.innovationnewsnetwork.com/bmw-brings-a-revolutionary-fleet-of-hydrogen-vehicles-to-our-roads/30656/

Transport

- **Shipping**

  - Hydrogen-derived fuels such as ammonia will likely be the most widely adopted option.

Proposed design of the vessel
Image credit: Nihon Shipyard

Heat and Building

- **Domestic heating**

- As the UK strives to meet its ambitious climate targets, decarbonizing the way we heat our homes and workplaces has become a key focus. Currently, heating accounts for nearly a quarter of the UK's carbon emissions, with around 85% of homes relying on natural gas. While technologies like heat pumps and heat networks are gaining traction, hydrogen heating is emerging as a potential alternative.

Hydrogen heating could be coming to the UK in 2026 based on the government's heating strategy *(Image credit: BDR Thermea)*

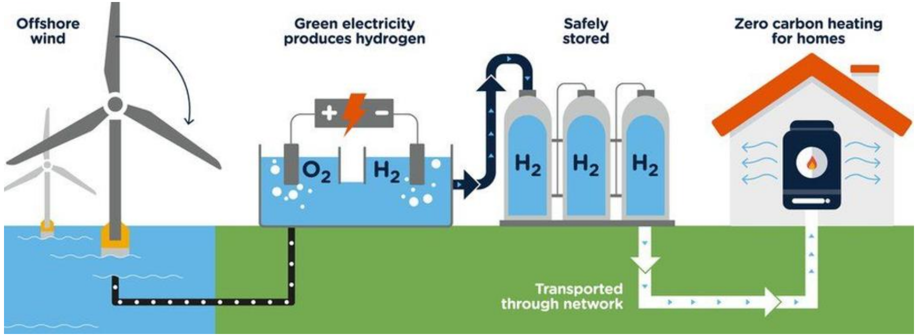

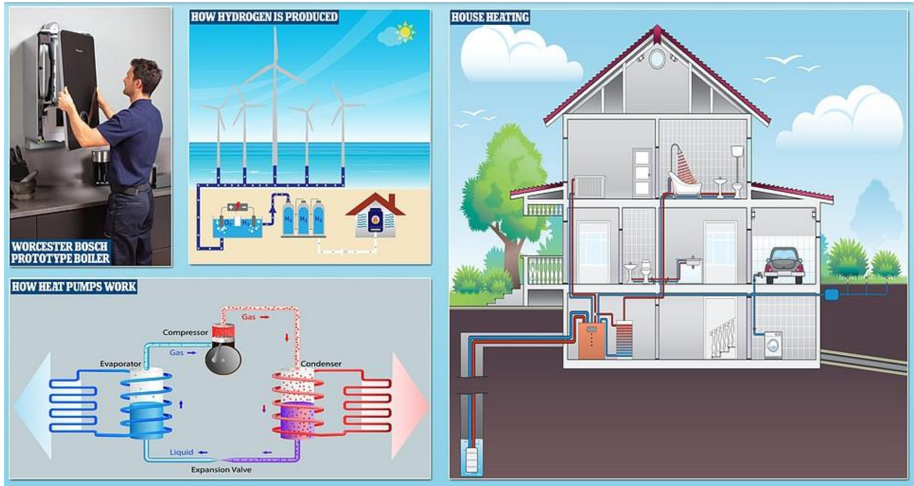

Sources: https://theicct.org/publication/hydrogen-for-heating-decarbonization-options-for-households-in-germany-in-2050/

AI Datacenter Power Solution

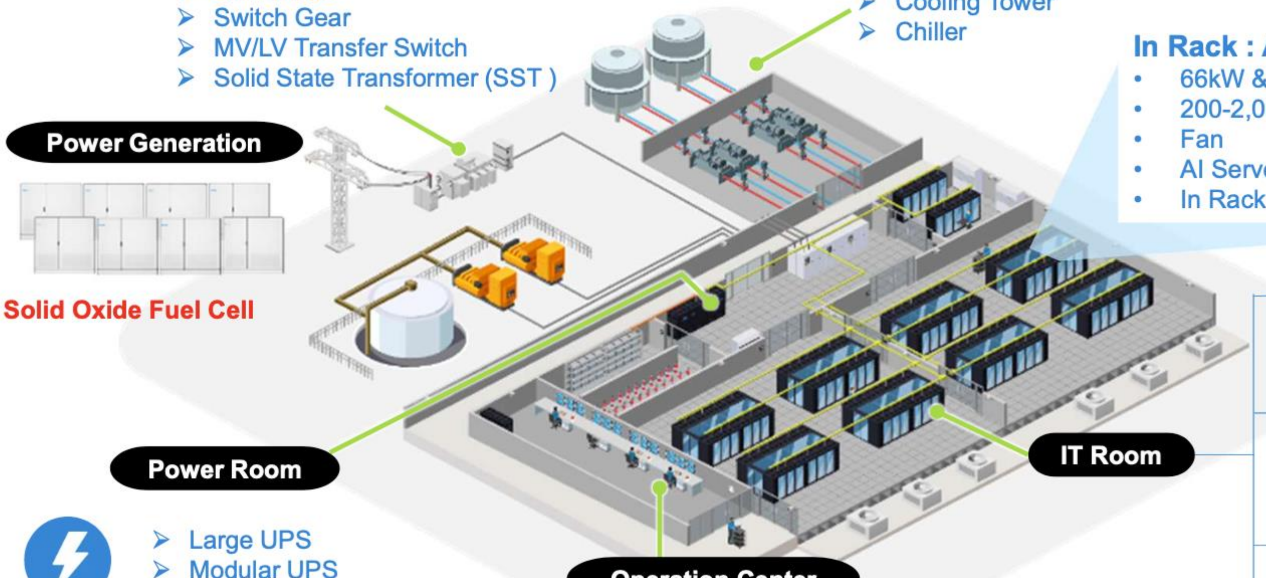

- Generator
- Switch Gear
- MV/LV Transfer Switch
- Solid State Transformer (SST)

- Cooling Tower
- Chiller

In Rack : AI Power & Thermal Management
- 66kW & 33kW Open Rack v3 Rack Mount Power Supply
- 200-2,000W , 48V/12V DC/DC Converter
- Fan
- AI Server GPU/CPU Cold Plate
- In Rack CDU (Coolant Distribution Unit)

- **Solid Oxide Fuel Cell**

Power Room
- Large UPS
- Modular UPS
- HVDC System
- STS
- PDU
- Busway

Operation Center
- DCIM
- Building Automation System
- Surveillance
- Video Wall
- Lighting

IT Room
- **OCP Rack**
- **Rack**

* IT Server/Storage

- Switch

- Modular UPS
- Rack level UPS
- 12 / 48VDC system
- rSTS
- rPDU
- Busway

- RowCool
- Rear Door Cooling
- Fan Wall
- Hot Aisle Containment System
- AALC
- Immersion Cooling

Benefits to Implement SOFC into Data Center as Primary Power

1. Lower CO_2 emission about -27% if no CCUS
2. Wider power sources options , easier for some countries those hard to have MW power supply

   A. Natural Gas

   B. Bio Gas

   C. Hydrogen

   D. Ammonia
3. Higher availability by having more energy sources to minimize the potential risk of single power sources failure .
4. High temperature fuel cell as SOFC to integrate with absorption cooling system for another energy saving
5. Possible to offer the DC power output direct to DC powered IT as stack originally generated DC power , higher efficiency

Attractiveness of Critical Load Users
Fuel Cell Distributed Prime Power Generation

Sustainability

- 40g CO_2 / kWh emission saving than Grid
- Energy saving with heat recycle and absorption cooling

Flexibility

- Multiple fuel options, Natural gas, Biogas, H2
- AC or DC power output
- Option to recycle the heat with absorption cooling
- 110kW per module, modular design for expansion

Time to Power

- 24 months to 9 months
- Optimized the cash flow of REIT/colocation builder

Reliability

- Distributed power generation to minimize the power outage of centralized grid
- Robust gas pipelines to minimize the disaster impact
- Easier buffer gas tank for long time backup

REIT : Real Estate Investment Trust

20Yrs Levelized Cost of Electricity (¢/kWh)

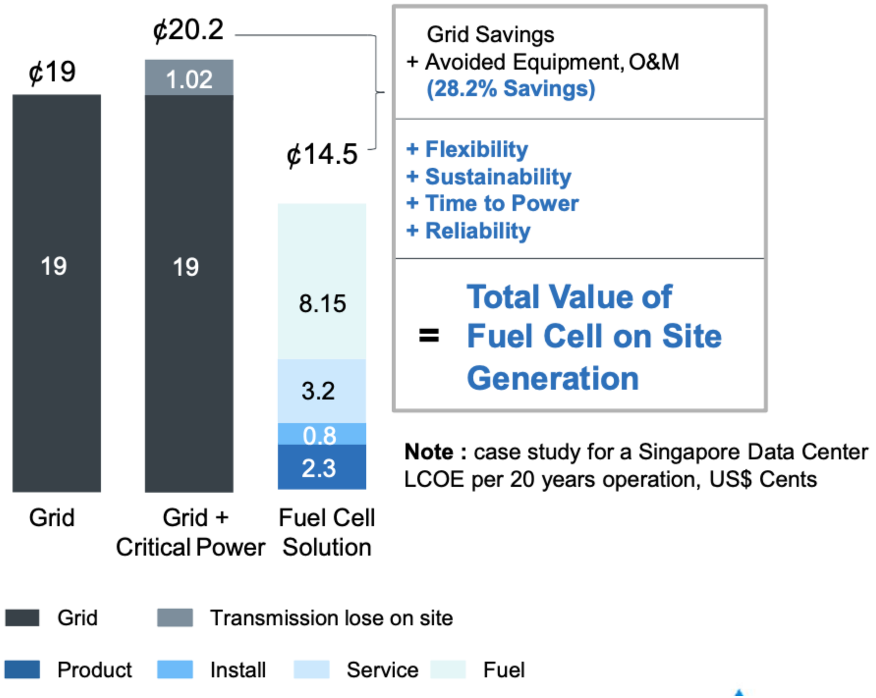

Benefits with SOFC as Primary Power in Data Center

- **Power Generation Sources Changed**

Scenario	Existing Power Architecture	SOFC Architecture
Primary Power	Utility	SOFC with Natural Gas
Short Term backup	UPS + Li-Ion Battery	UPS + Li-Ion Battery
Backup power	Diesel Generator	Utility

- **Advantages**

1. **Minimize the potential outage of centralized power generation**
2. **Time to get power permission**
3. **Same site to expand for higher power density**
4. **Eliminate the diesel generator**
5. **Lower CO_2 emission**
6. **Heat recycle with Absorption Chiller**

Delta's Target Technology & Application

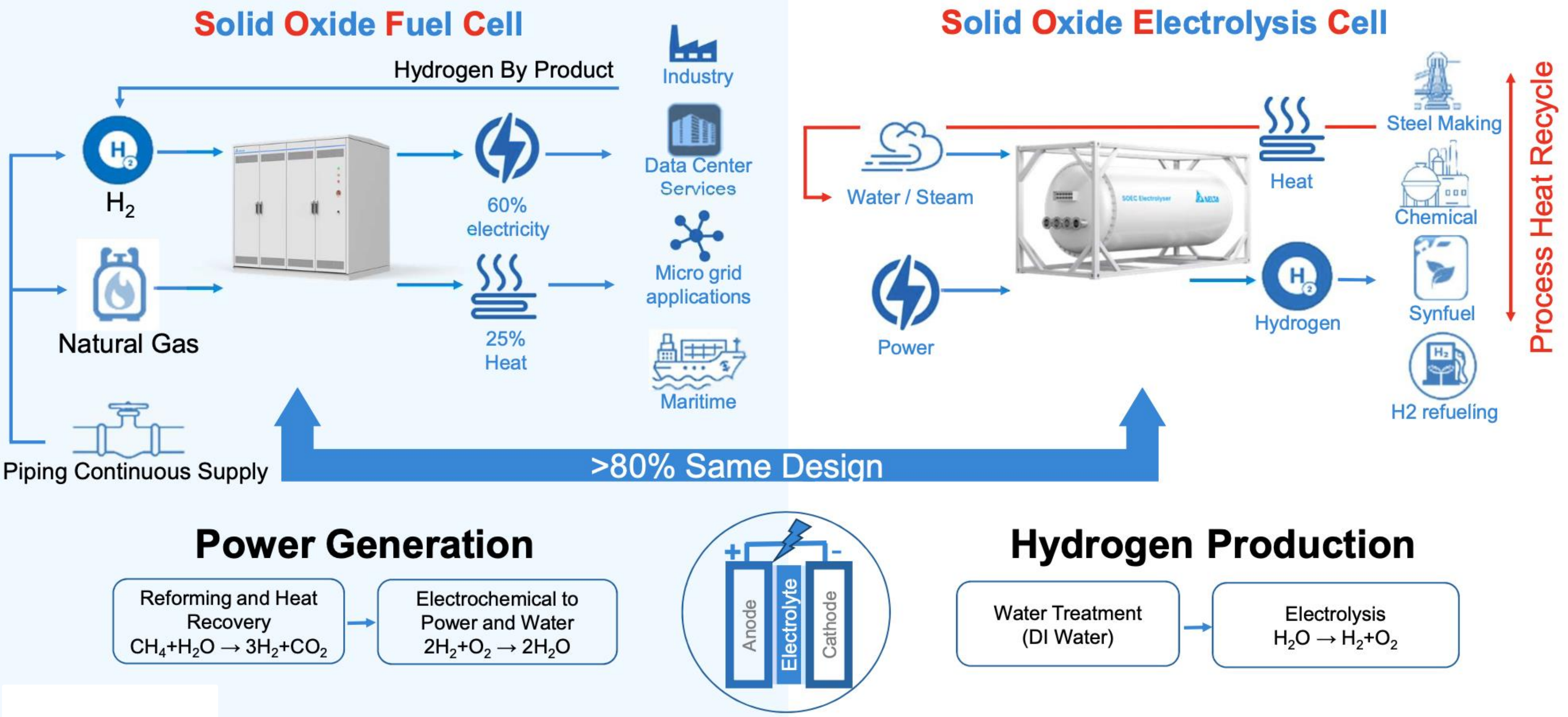

Modular Design - Capacity Expanded

C&I 550kW System

1.1MW Centralized System

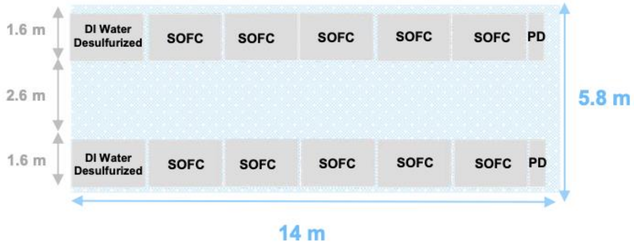

5.5MW Centralized System

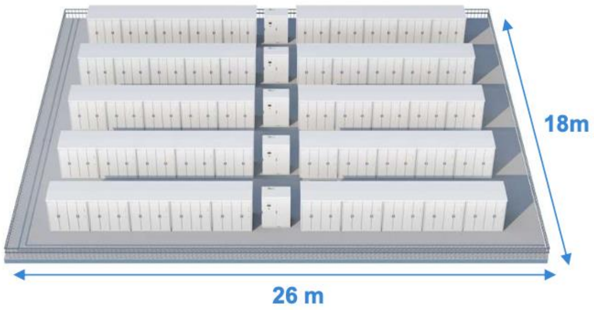

25MW Power Tower Concept

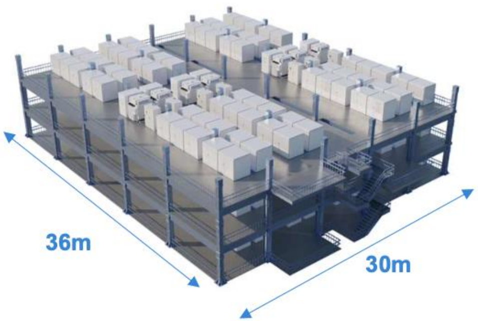

Key Messages

Fuel Options	• Natural Gas • Hydrogen (H2) – Future model • Ammonia (NH3) – Future model
Efficiency (LHV)	• 53% ~ 63% (Electricity Generation)
Life	• Stack : >40KHrs (EOL: LHV > 53%) · Capable for operation after 40Khrs • System : >15 Years
Continues Operation	• 24/7 non-stop and continues power generation • Capacity factor > 95%
Fuel Consumption	• Natural Gas 1M³ = about 5.5kWh
CO_2 Emission Intensity	• <360g/kWh (fuel as natural gas)
After Service	• 1st year as free warranty upon handover • Service level agreement from 2nd years onwards

Delta Net Zero Science Lab


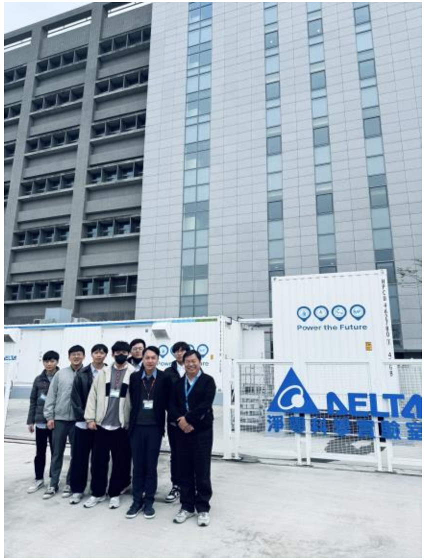

Delta, a global leader in power management and a provider of IoT-based smart green solutions, inaugurated today Taiwan's 1st megawatt (MW)-grade R&D lab for water electrolysis hydrogen production and for fuel cells, the "Delta Net Zero Science Lab," at its Tainan Plant 2. This significant milestone provides a diverse testing environment for component and system validation of hydrogen production and fuel cell technologies.

Comparison of Solid Oxide Fuel Cell Types

- SOFC have advantages such as **high energy efficiency**, **fuel flexibility**, and **low environmental impact**.

	TSOFC (Tubular SOFC)	CS-SOFC and AS-SOFC (Cathode-Supported SOFC, Anode-Supported SOFC)	ES-SOFC (Electrolyte-Supported SOFC)	MS-SOFC (Metal-Supported SOFC)
Advantage	• Good sealing • More robust and stable structure • Stronger thermal cycling capability	• Lowering the internal resistance • Lower temperatures	• Simplify the battery structure. • Better long-term stability	• Enhance structural strength • Resistance to thermal stress. • Electrode thickness • Better thermal conductivity
Defect	• Complex manufacturing processes • Higher costs • Higher internal resistance • Lower efficiency.	• Longer startup time • Special structure and materials • The current density of CS-SOFC is lower than that of AS-SOFC.	• higher internal resistance • lower efficiency • relatively low structural strength	• Fuel corrosion • Special materials treatment and design

Emerging **MS-SOFC** designs offer several important advantages over traditional designs, including lower-to-medium operating temperatures, enhanced thermal response capabilities, and shorter startup times.
They are thus considered to have significant commercial potential. However, their performance under different fuel conditions is not yet clear.

1. Accordingly, in recent research, **stack model simulations** were performed to investigate the current density, voltage, temperature distribution, and fuel cell fractions in a typical **MS-SOFC** design operated with either pure hydrogen fuel or mixed fuel with various **water-to-carbon ratios (S/C)** and methane vapor reforming reaction rates.

2. The purpose of the **simulations** was to establish the operating parameters that optimized the current density and overall performance of the MS-SOFC under **low-temperature conditions of 600 °C**.

SOFC System

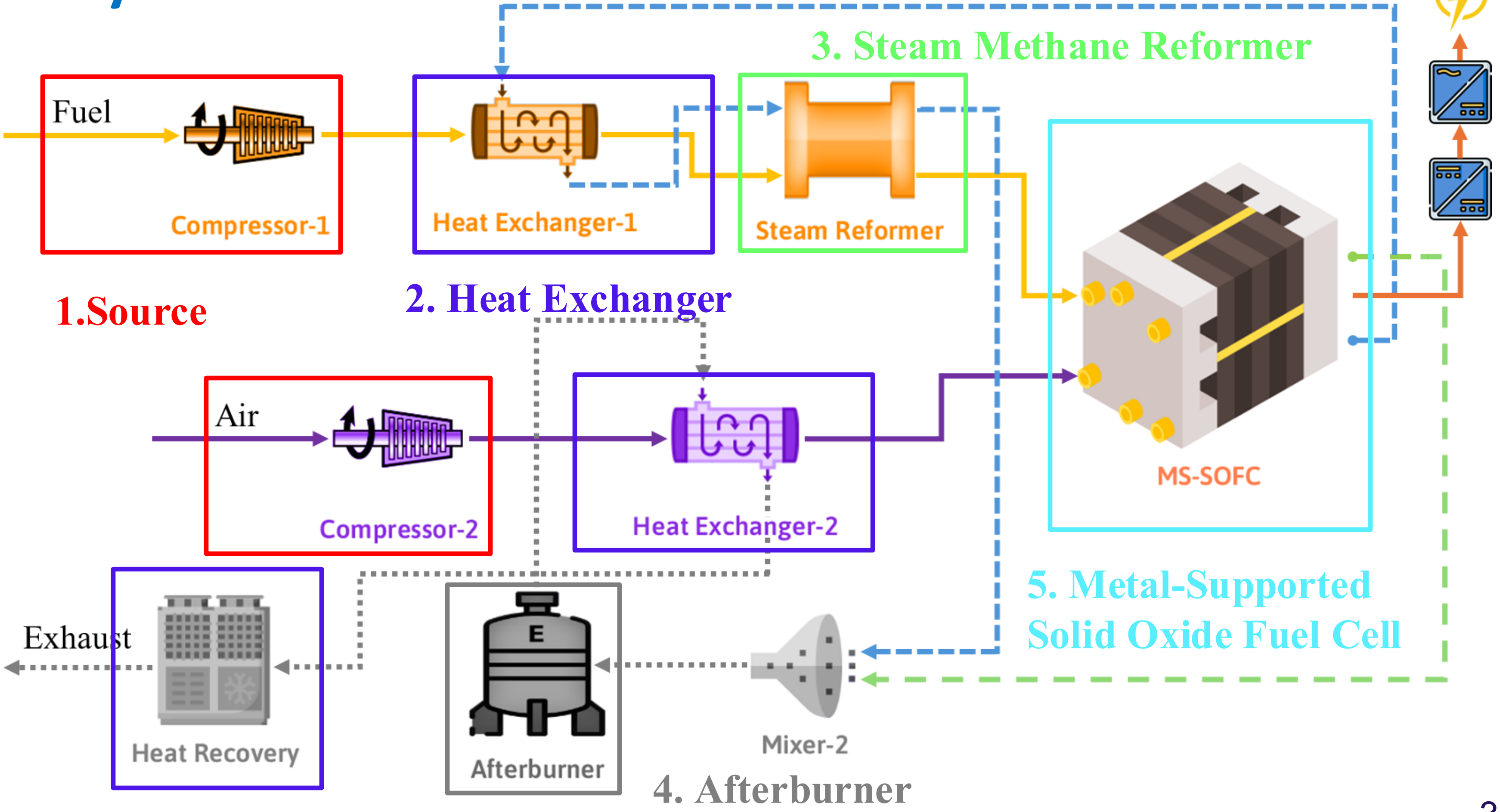
3. Steam Methane Reformer
Fuel
Compressor-1
Heat Exchanger-1
Steam Reformer
1.Source
2. Heat Exchanger
Air
Compressor-2
Heat Exchanger-2
MS-SOFC
5. Metal-Supported
Solid Oxide Fuel Cell
Exhaust
Heat Recovery
E
Afterburner
Mixer-2
4. Afterburner

MS-SOFC

Mass balances

1. Fuel Channel
2. Air Channel
3. Chemical Reaction

Energy balances

1. Fuel Channel
2. Air Channel
3. PEN structure
4. Interconnect

Electrochemical

1. Nernst equation
2. Ohmic Overpotential
3. Concentration Polarization
4. Activation loss

Other components

Source

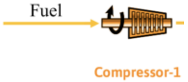

Ideal gas law

Peng-Robinson Equation of State (PR-EOS)

Reformer
Afterburner

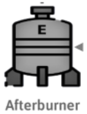

Equilibrium reactor

Energy balance

Mass balance

Heater
Heat Exchanger

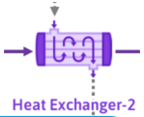

Energy balance

Mass balance

Mass balances

1. Fuel Channel

Concentration of Fuel Channel

$$\frac{\partial C_{i,f}}{\partial t} = -u_f \frac{\partial C_{i,f}}{\partial x} + \sum_{k\epsilon\{(i),(ii),(V)\}} v_{i,k} R_{i,k} \frac{1}{h_f}$$

$i \epsilon \{CH_4, H_2O, CO, H_2, CO_2\}$

$C_{i,f}$: molar concentration of component

Concentration

$$PV = nRT \,, C = \frac{n}{V}$$

$$\Rightarrow C = \frac{n}{V} = \frac{P_i}{R * T_{an}} = \frac{P_{an} * f_i}{R * T_{an}}$$

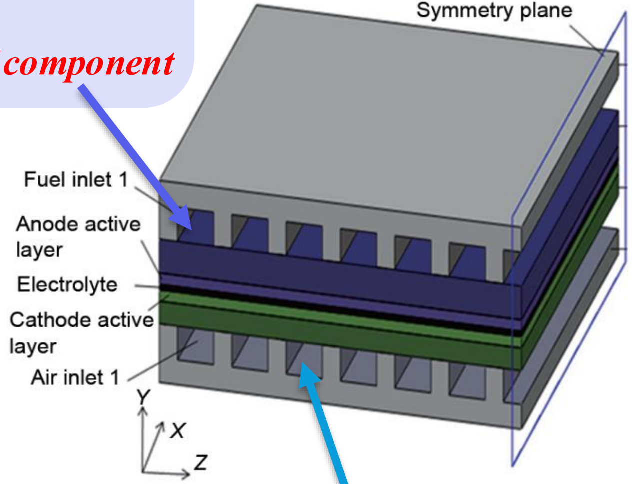

2. Air Channel

$$\frac{\partial C_{i,a}}{\partial t} = -u_a \frac{\partial C_{i,a}}{\partial x} + v_{i,(V)} R_{i,(V)} \frac{1}{h_a} \quad , i \epsilon \{O_2, N_2\}$$

Concentration of Air Channel

3. Chemical Reaction

(i). Electrochemical

$$R_{(i)} = \frac{j}{2F}$$

(ii). Steam Reforming

$$R_{(ii)} = k_0 p_{CH_4} \exp\left(-\frac{E_a}{RT}\right)$$

(iii). Gas-shift

$$R_{(iii)} = k_{WGSR} p_{CO} (1 - \frac{p_{CO_2} p_{H_2} / p_{CO} p_{H_2O}}{RT})$$

Energy balances

Two-Phase (Solid-Gas)

1. Fuel Channel

Temperature of Anode

$$\rho_f c_{p,f}\frac{\partial T_f}{\partial t} = -u_f\rho_f c_{p,f}\frac{\partial T_f}{\partial x} + k_{f,PEN}(T_{PEN}-T_f)\frac{1}{h_f} + k_{f,I}(T_{PEN}-T_f)\frac{1}{h_f} + \Sigma\ (-\Delta H)_k R_k\frac{1}{h_f}$$

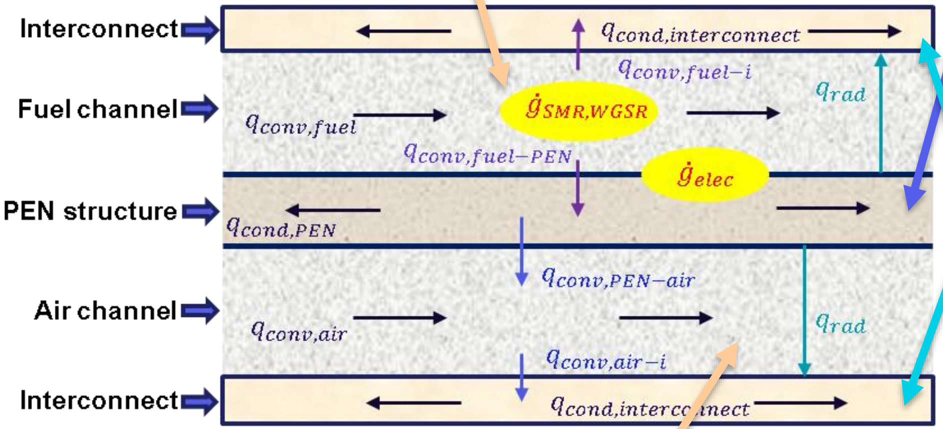

2. Air Channel

$$\rho_a c_{p,a}\frac{\partial T_a}{\partial t} = -u_a\rho_a c_{p,a}\frac{\partial T_a}{\partial x} + k_{a,PEN}(T_{PEN}-T_a)\frac{1}{h_a} + K_{a,I}(T_I-T_a)\frac{1}{h_a}$$

Temperature of Cathode

3. PEN structure

PEN :Positive-electrode/Electrolyte/Negative-electrode

$$\rho_{PEN}c_{p,PEN}\frac{\partial T_{PEN}}{\partial t} = \lambda_{PEN}\frac{\partial^2 T_{PEN}}{\partial x^2} - k_{f,PEN}(T_{PEN}-T_f)\frac{1}{\tau_{PEN}}$$

Temperature of PEN structure

$$-k_{a,PEN}(T_{PEN}-T_a)\frac{1}{\tau_{PEN}} + [(-\Delta H)_{(v)}R_{(v)} - jU]\frac{1}{\tau_{PEN}} + \left[\frac{\sigma(T_I^4 - T_{PEN}^4)}{\frac{1}{\epsilon_1}+\frac{1}{\epsilon_{PEN}}-1}\right]\frac{1}{\tau_{PEN}}$$

4. Interconnect

Temperature of Interconnect

$$\rho_I c_{p,I}\frac{\partial T_I}{\partial t} = \lambda_I\frac{\partial^2 T_I}{\partial x^2} - k_{f,I}(T_I-T_f)\frac{1}{\tau_I} - k_{a,I}(T_I-T_a)\frac{1}{\tau_I} - \left[\frac{\sigma(T_I^4 - T_{PEN}^4)}{\frac{1}{\epsilon_1}+\frac{1}{\epsilon_{PEN}}-1}\right]\frac{1}{\tau_I}$$

Specific heat capacity

$$c_{p,ca} = 0.92 f_{O_2} + 1.04 f_{N_2}$$

$$c_{p,an} = 14.3 f_{H_2} + 2.156 f_{H_2} 2.156 f_{CH_4} 2.21 f_{CO} + 0.8 f_{CO_2}$$

Density of the gas steams

$$PV = nRT = \frac{m}{M}RT \longrightarrow \rho_{an} = \frac{m}{V} = \frac{PM}{RT} = \sum \frac{P_i M_i}{RT_{an}}$$

Electrochemical

$$U = U_{TPB}^{OCP} - (\eta_{Ohm} + \eta_{conc,anode} + \eta_{conc,cathode} + \eta_{act,anode} + \eta_{act,cathode})$$

TPB : Three-Phase Boundaries

Nernst equation

$$U_{TPB}^{OCP} = U_{H_2}^{0} - \frac{RT}{2F} \ln\left(\frac{p_{H_2O,TPB}}{p_{H_2,TPB}\, p_{O_2,TPB}^{0.5}}\right)$$

$$p_{H_2,TPB} = p_{H_2,f} - \frac{RT\tau_{anode}}{2FD_{eff,anode}} j$$

Gas distribution diagram at the three-phase boundary in SOFC

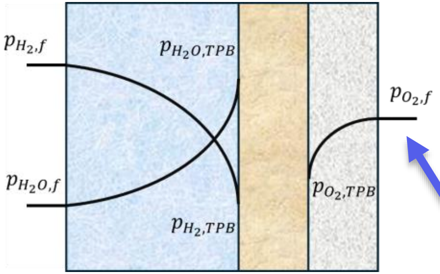

$$p_{O_2,TPB} = P - (P - p_{O_2,a}) - \frac{RT\tau_{anode}}{4FD_{eff,cathode}P} j$$

$$p_{H_2O,TPB} = p_{H_2O,f} - \frac{RT\tau_{anode}}{2FD_{eff,anode}} j$$

Polarization

Ohmic Overpotentials

$$\eta_{Ohm} = jR_{Ohm} \quad , R_{Ohm} = \frac{\tau_{anode}}{\sigma_{anode}} + \frac{\tau_{electrolyte}}{\sigma_{electrolyte}} + \frac{\tau_{cathode}}{\sigma_{cathode}}$$

Concentration Polarization

$$\eta_{conc} = \frac{RT}{2F} \ln\left(\frac{p_{H_2O,TPB}\, p_{H_2,f}}{p_{H_2,TPB}\, p_{H_2O,f}}\right) + \frac{RT}{4F} \ln\left(\frac{p_{O_2,a}}{p_{O_2,TPB}}\right)$$

Activation loss

$$j = j_{0,electrode}\left[\exp\left(\frac{\alpha nF}{RT}\eta_{act,elect}\right) - \exp\left(\frac{(1-\alpha)nF}{RT}\eta_{act,elect}\right)\right]$$

$$j_{0,electrode} = \frac{RT}{2F} k_{electrode} \exp\left(\frac{E_{electrode}}{RT}\right)$$

Other components

Steam Methane Reformer and Afterburner

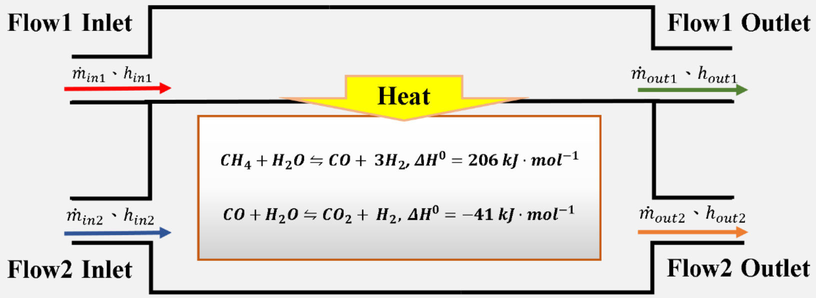

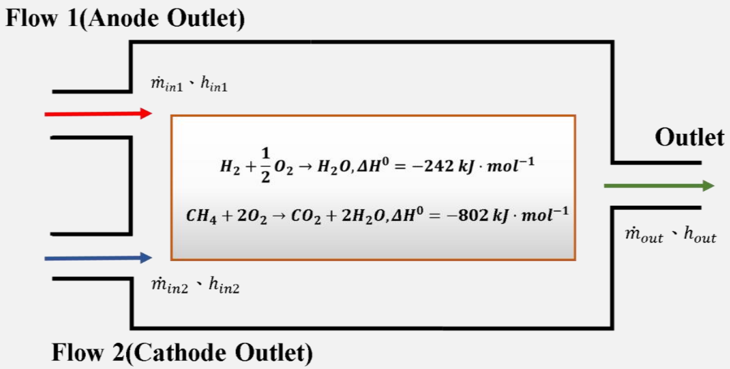

Equilibrium reactor: General chemical reaction formula: $aA + bB \leftrightharpoons cC + dD$

Equilibrium constant $ln(k) = \frac{\Delta G}{RT}$ ⇒ $k = \left(\frac{\Psi_C^c \cdot \Psi_D^d}{\Psi_A^a \cdot \Psi_B^b}\right) \cdot \left(\frac{p}{p_0}\right)^{\Delta n}$ ⇒ Ψ: *mole fractions of each species at equilibrium in a chemical reaction*

Mass balance $\frac{dm}{dt} = \sum \dot{m}_{out} - \sum \dot{m}_{in}$

Energy balance $\frac{dU}{dt} = \sum \dot{H}_{in,i} + \sum \dot{H}_{out,i} + \sum \dot{Q}_k$

$\Delta G = Gibbs\ free\ energy\ changes$

Other components

Source

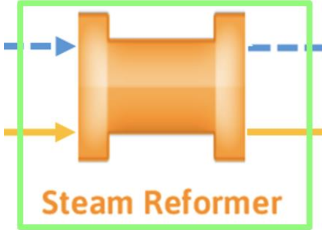

$$Z \times R \times T = p \times v$$

- **Z=1, ideal gas**
- **Z≠1, Peng-Robinson Equation of State, PR-EOS**

$$P = \frac{RT}{V_m - b} - \frac{a\alpha}{V_m^2 + 2bV_m - b^2}$$

$$a = \frac{0.4572 R^2 T_c^2}{P_c}$$

$$b = \frac{0.0778 R T_c}{P_c}$$

$$Z^3 - (1 - B)Z^2 + (A - 2B - 3B^2)Z - (AB - B^2 - B^3) = 0$$

$$A = \frac{a\alpha P}{R^2 T^2}, B = \frac{bP}{RT}$$

$$Z = \frac{PV}{RT}$$

- Z = Compressibility factor
- α = Non-ideal quadratic correction parameters
- V_m = molar volume of gas
- T_c = Critical Temperature
- P_c = Critical Pressure

Steam Methane Reformer and Afterburner

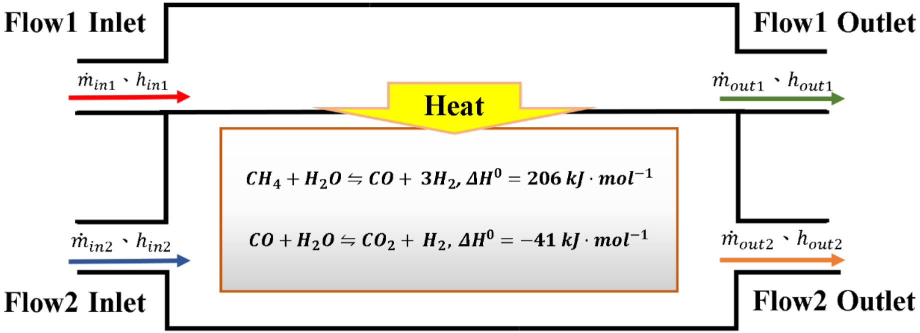

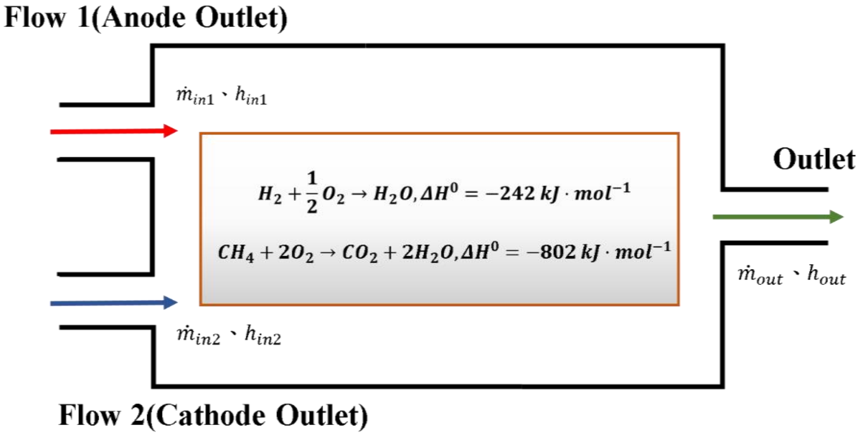

Other components

Heater and Heat Exchanger

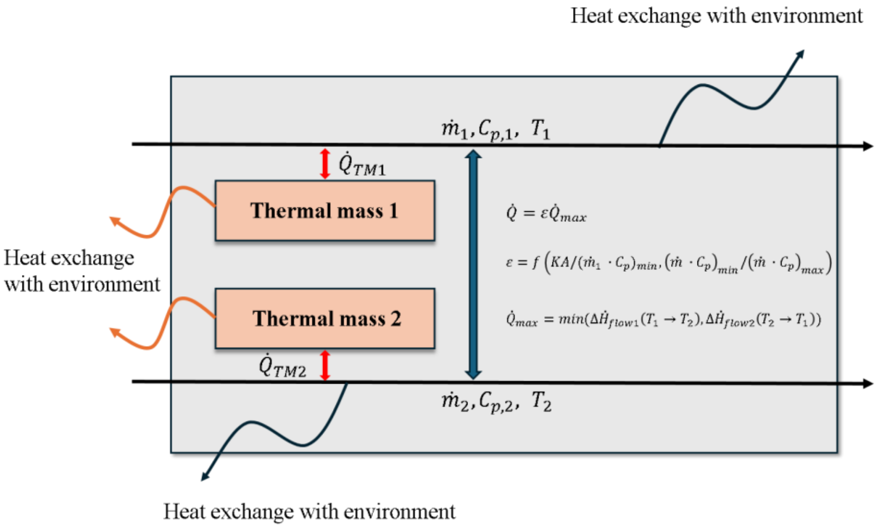

Counter flow:

$$\varepsilon = \left(\frac{1 - exp(-N(1 - C))}{1 - C}\right)$$

$$NTU = \frac{UA}{\dot{C}_{min}}, \; C = \frac{\dot{C}_{min}}{\dot{C}_{max}}$$

Solution steps:

Step1.

$$\dot{C}_{min} = min(\dot{m}_1 C_{p1}, \dot{m}_2 C_{p2})$$

$$\dot{C}_{max} = max(\dot{m}_1 C_{p1}, \dot{m}_2 C_{p2})$$

Step2.

$$\dot{Q}_{max} = \dot{C}_{min}(T_{hi} - T_{ci})$$

Step3.

$$\dot{Q} = \varepsilon \dot{Q}_{max}$$

Step4.

$$T_{1,out} = T_{1,out} - \frac{\dot{Q}}{\dot{m}_1 C_{p1}}$$

$$T_{2,out} = T_{2,out} - \frac{\dot{Q}}{\dot{m}_2 C_{p2}}$$

Final verification and judgment

$$\dot{Q}_{TM,env} = sign(\dot{Q}_{env}) \times min(|\dot{Q}_{env}|, |h_{flow}(T_i) - h_{flow}(T_{env})|)$$

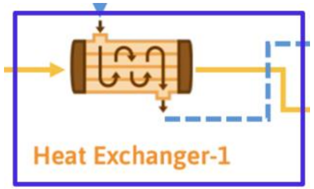

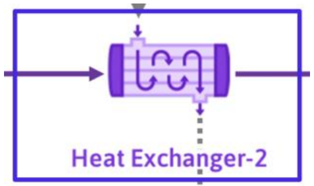

3. Simulink Modeling

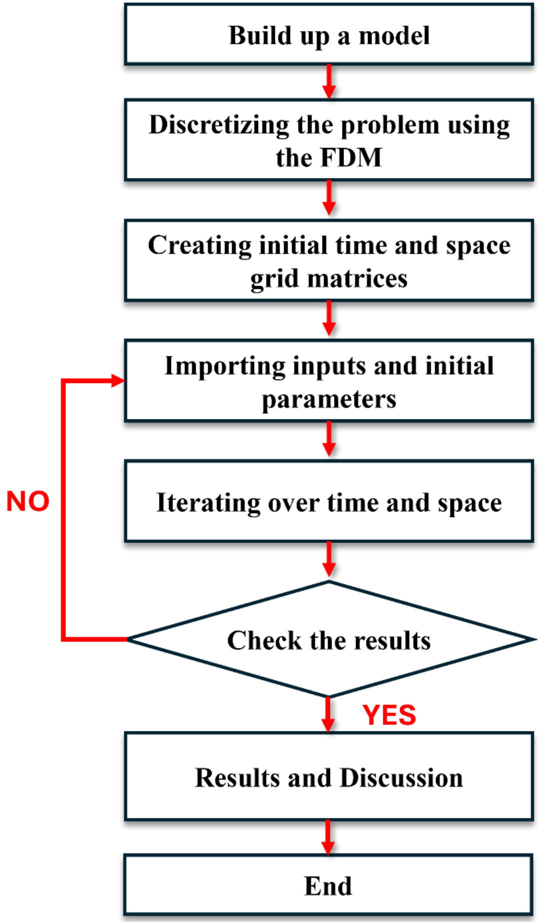

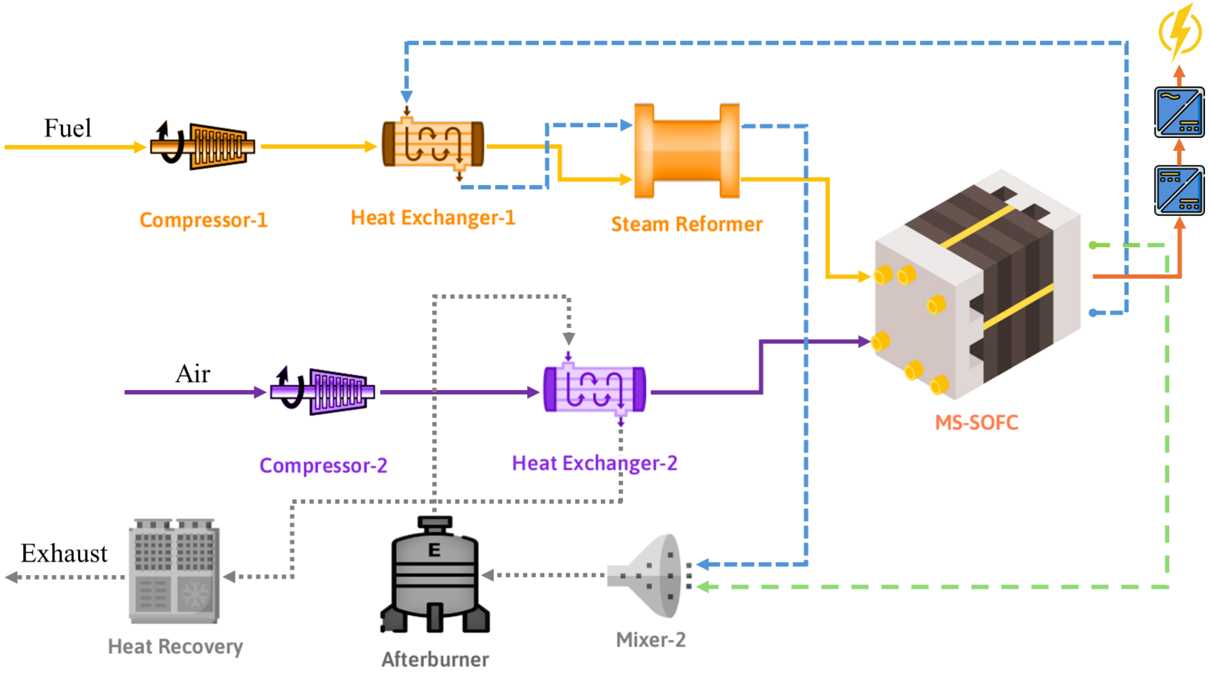

Framework of MS-SOFC system simulations using finite difference method

Finite difference methods

1. Convection equation

- Mass balances of Fuel channel
- Mass balances of Air channel
- Energy balance of Fuel channel
- Energy balance of Air channel

$$\frac{\partial u}{\partial t} = D\frac{\partial^2 u}{\partial x^2}$$

$$D\frac{\partial^2 u}{\partial x^2}(x_j,t_n) + f(x_j,t_n)$$

$$u(x_j,t_n+\Delta t) = u(x_j,t_n) + \frac{\partial u}{\partial t}(x_j,t_n)\Delta t + \frac{1}{2}\frac{\partial^2 u}{\partial t^2}(x_j,t_n)\Delta t^2 + \cdots u(t^4)$$

$$u(x_j+\Delta x,t_n) = u(x_j,t_n) + \frac{\partial u}{\partial x}(x_j,t_n)\Delta x + \frac{1}{2}\frac{\partial^2 u}{\partial x^2}(x_j,t_n)\Delta x^2 + \cdots u(x^4)$$

$$u(x_j-\Delta x,t_n) = u(x_j,t_n) - \frac{\partial u}{\partial x}(x_j,t_n)\Delta x + \frac{1}{2}\frac{\partial^2 u}{\partial x^2}(x_j,t_n)\Delta x^2 - \cdots u(x^4)$$

$$\frac{\partial C_{i,f}}{\partial t} = -u_f\frac{\partial C_{i,f}}{\partial x}$$

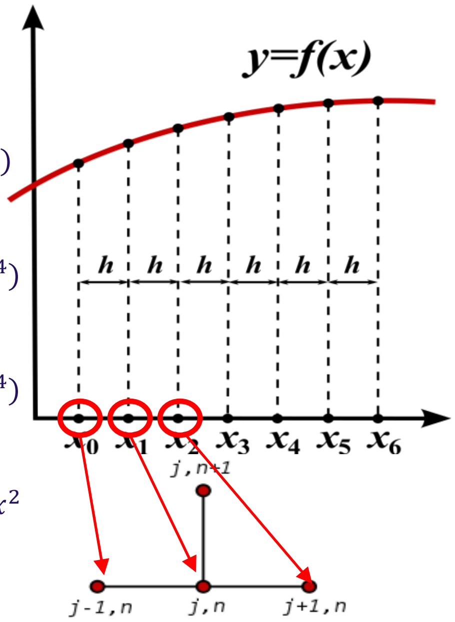

2. Diffusion equation

$$\frac{\partial^2 u}{\partial x^2}(x_j,t_n) = [u(x_j+\Delta x,t_n) + u(x_j-\Delta x,t_n) - 2u(x_j,t_n) + \cdots u(x^4)]/\Delta x^2$$

- Energy balance of PEN structure
- Energy balance of Interconnect

$$\frac{\partial^2 u}{\partial x^2}(x_j,t_n) \approx \frac{u_{j+1}^n - 2u_j^n + u_{j-1}^n}{\Delta x^2}$$

$$\rho_I c_{p,I}\frac{\partial T_I}{\partial t} = \lambda_I\frac{\partial^2 T_I}{\partial x^2}$$

$$u_j^{n+1} = u_j^n + \left[D\frac{u_{j+1}^n - 2u_j^n + u_{j-1}^n}{\Delta x^2} + f_j^n\right]\Delta t$$

Discretization : $x_j = x_0 + (j-1)dx$

$$t_n = 0 + (n-1)dt$$

$$dx = \frac{x_n - x_0}{\mathrm{N}}$$

Finite difference methods

MS-SOFC

$$\frac{\partial C_{i,f}}{\partial t} = -u_f \frac{\partial C_{i,f}}{\partial x} + \sum_{k\epsilon\{(i),(ii),(V)\}} v_{i,k} R_{i,k} \frac{1}{h_f}$$

The Concentration at the Next Time Step

$$C_{i,j}^{n+1} = C_{i,j}^{n} + dt * \left(-u_f \frac{C_{i,j}^{n} - C_{i,j-1}^{n}}{dx} + \sum_{k\epsilon\{(i),(ii),(V)\}} v_{i,k} R_{i,k} \frac{1}{h_f}\right)$$

The Current Spatial Step and its Impact Factors

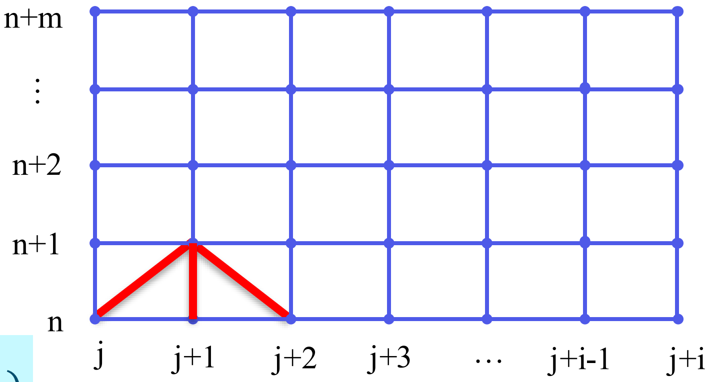

Finite Finite Difference approximations

$$\rho_{PEN} c_{p,PEN} \frac{\partial T_{PEN}}{\partial t} = \lambda_{PEN} \frac{\partial^2 T_{PEN}}{\partial x^2} - k_{f,PEN}(T_{PEN} - T_f)\frac{1}{\tau_{PEN}} - k_{a,PEN}(T_{PEN} - T_f)\frac{1}{\tau_{PEN}} + [(-\Delta H)_{(v)} R_{(v)} - jU]\frac{1}{\tau_{PEN}} + [\frac{\sigma(T_I^4 - T_{PEN}^4)}{\frac{1}{\epsilon_1} + \frac{1}{\epsilon_{PEN}} - 1}]\frac{1}{\tau_{PEN}}$$

The Temperature at the Next Time Step

$$T_{PEN,j}^{n+1} = T_{PEN,j}^{n} + \frac{dt}{\rho_{PEN} c_{p,PEN}}\left(\lambda_{PEN} \frac{T_{PEN,j+1}^{n} - 2T_{PEN,j}^{n} + T_{PEN,j-1}^{n}}{dx^2} - k_{f,PEN}(T_{PEN,j} - T_{f,j})\frac{1}{\tau_{PEN}} - k_{a,PEN}(T_{PEN,j} - T_{,j})\frac{1}{\tau_{PEN}} + \cdots\right)$$

The Current Spatial Step and its Impact Factors

Model code

1. Parameter setting

```
% Parameter of mesh
L = 0.24;
dx = 0.04;
dt = 0.004;
x  = 0:dx:L;

W          = 0.1;
h_an       = 0.001;     %fuel channel height(m)


%molar flow Rate_anode
ndot_H2     = n_in_H2/Number_cell;
ndot_H2O    = n_in_H2O/Number_cell;
ndot_CH4    = n_in_CH4/Number_cell;
ndot_CO     = n_in_CO/Number_cell;
ndot_CO2    = n_in_CO2/Number_cell;
ndot_N2    = n_in_N2/Number_cell;

Pan_out     = Pan;

CD          = i/length(x)/(W*dx);
R           = 8.314;
F           = 96485;
k0          = 4274;
k_WGSR      = 0.1;
Ea          = 82;
```

2. Zero matrix

```
%%
% 初始化結果矩陣_anode
u1 = zeros(length(x),2);
u2 = zeros(length(x),2);
u3 = zeros(length(x),2);
u4 = zeros(length(x),2);
u5 = zeros(length(x),2);
u6 = zeros(length(x),2);

u1_2 = zeros(length(x),2);
u2_2 = zeros(length(x),2);

ndot_out_H2  = zeros(length(x),1);
ndot_out_H2O = zeros(length(x),1);
ndot_out_CH4 = zeros(length(x),1);
ndot_out_CO  = zeros(length(x),1);
ndot_out_CO2 = zeros(length(x),1);
ndot_out_N2  = zeros(length(x),1);

P1 = zeros(length(x),1);
P2 = zeros(length(x),1);
P3 = zeros(length(x),1);
P4 = zeros(length(x),1);
P5 = zeros(length(x),1);
```

3. Initial value setting

```
%Concentration calculation_anode
C1 = (Pan*ndot_H2) /(8.2057e-5*T_an_in*(ndot_H2+ndot_H2O+ndot_CH4+ndot_CO+ndot_CO2));
C2 = (Pan*ndot_H2O)/(8.2057e-5*T_an_in*(ndot_H2+ndot_H2O+ndot_CH4+ndot_CO+ndot_CO2));
C3 = (Pan*ndot_CH4)/(8.2057e-5*T_an_in*(ndot_H2+ndot_H2O+ndot_CH4+ndot_CO+ndot_CO2));
C4 = (Pan*ndot_CO) /(8.2057e-5*T_an_in*(ndot_H2+ndot_H2O+ndot_CH4+ndot_CO+ndot_CO2));
C5 = (Pan*ndot_CO2)/(8.2057e-5*T_an_in*(ndot_H2+ndot_H2O+ndot_CH4+ndot_CO+ndot_CO2));
C6 = (Pan*ndot_N2)/(8.2057e-5*T_an_in*(ndot_H2+ndot_H2O+ndot_CH4+ndot_CO+ndot_CO2));

u_an = (ndot_H2+ndot_H2O+ndot_CH4+ndot_CO+ndot_CO2)/((C1+C2+C3+C4+C5)*(W*h_an));
%%

matrix_H2  = (Pan*matrix_in_H2) ./(8.2057e-5*T_an_x.*(matrix_in_H2+matrix_in_H2O+matrix_in_CH4+matrix_in_CO+matrix_in_CO2+matrix_in_N2));
matrix_H2O = (Pan*matrix_in_H2O)./(8.2057e-5*T_an_x.*(matrix_in_H2+matrix_in_H2O+matrix_in_CH4+matrix_in_CO+matrix_in_CO2+matrix_in_N2));
matrix_CH4 = (Pan*matrix_in_CH4)./(8.2057e-5*T_an_x.*(matrix_in_H2+matrix_in_H2O+matrix_in_CH4+matrix_in_CO+matrix_in_CO2+matrix_in_N2));
matrix_CO  = (Pan*matrix_in_CO) ./(8.2057e-5*T_an_x.*(matrix_in_H2+matrix_in_H2O+matrix_in_CH4+matrix_in_CO+matrix_in_CO2+matrix_in_N2));
matrix_CO2 = (Pan*matrix_in_CO2)./(8.2057e-5*T_an_x.*(matrix_in_H2+matrix_in_H2O+matrix_in_CH4+matrix_in_CO+matrix_in_CO2+matrix_in_N2));
matrix_N2 = (Pan*matrix_in_N2)./(8.2057e-5*T_an_x.*(matrix_in_H2+matrix_in_H2O+matrix_in_CH4+matrix_in_CO+matrix_in_CO2+matrix_in_N2));

%The input matrix from the previous time step
u1(:, 1) = matrix_H2;
u2(:, 1) = matrix_H2O;
u3(:, 1) = matrix_CH4;
u4(:, 1) = matrix_CO;
u5(:, 1) = matrix_CO2;
u6(:, 1) = matrix_N2;

%Boundary_H2_H2O_CH4_CO_CO2
u1(1,1) = C1 ;
u2(1,1) = C2 ;
u3(1,1) = C3 ;
u4(1,1) = C4 ;
u5(1,1) = C5 ;
u6(1,1) = C6 ;
```

4. Calculate value iteration

```
for n = 1
    for j = 1:length(x)-1

        f1(f1 < 0 | isnan(f1)) = 0;
        f2(f2 < 0 | isnan(f2)) = 0;
        f3(f3 < 0 | isnan(f3)) = 0;

        u1(j+1,n+1) = u1(j+1, n) - ((dt*u_an/dx)*(u1(j+1, n) - u1(j, n)))+dt/h_an*(+3*f2(j+1,n)+1*f3(j+1,n));
        u2(j+1,n+1) = u2(j+1, n) - ((dt*u_an/dx)*(u2(j+1, n) - u2(j, n)))+dt/h_an*(-1*f2(j+1,n)-1*f3(j+1,n));
        u3(j+1,n+1) = u3(j+1, n) - ((dt*u_an/dx)*(u3(j+1, n) - u3(j, n)))+dt/h_an*(-1*f2(j+1,n)+0*f3(j+1,n));
        u4(j+1,n+1) = u4(j+1, n) - ((dt*u_an/dx)*(u4(j+1, n) - u4(j, n)))+dt/h_an*(+1*f2(j+1,n)-1*f3(j+1,n));
        u5(j+1,n+1) = u5(j+1, n) - ((dt*u_an/dx)*(u5(j+1, n) - u5(j, n)))+dt/h_an*(+0*f2(j+1,n)+1*f3(j+1,n));
        u6(j+1,n+1) = u6(j+1, n) - ((dt*u_an/dx)*(u6(j+1, n) - u6(j, n)))+dt/h_an*(+0*f2(j+1,n)+0*f3(j+1,n));

        u1_2(j+1,n+1) = u1(j+1,n+1)+dt/h_an*(-1*f1(j+1,n));
        u2_2(j+1,n+1) = u2(j+1,n+1)+dt/h_an*(+1*f1(j+1,n));

        if u1(j+1,n+1)<=0
            f1(j+1,n)=0;
        else
            f1(j+1,n)=f1(j+1,n);
        end

    end
end
```

5. Calculated value output

```
ndot_out_H2(:,1)   = u1(:,1)*u_an*(W*h_an)*Number_cell;
ndot_out_H2O(:,1)  = u2(:,1)*u_an*(W*h_an)*Number_cell;
ndot_out_CH4(:,1)  = u3(:,1)*u_an*(W*h_an)*Number_cell;
ndot_out_CO(:,1)   = u4(:,1)*u_an*(W*h_an)*Number_cell;
ndot_out_CO2(:,1)  = u5(:,1)*u_an*(W*h_an)*Number_cell;
ndot_out_N2(:,1)   = u6(:,1)*u_an*(W*h_an)*Number_cell;

n_out_H2    = ndot_out_H2(end,1);
n_out_H2O   = ndot_out_H2O(end,1);
n_out_CH4   = ndot_out_CH4(end,1);
n_out_CO    = ndot_out_CO(end,1);
n_out_CO2   = ndot_out_CO2(end,1);
n_out_N2   = ndot_out_N2(end,1);
```

Self-written program code

Simulink Modeling

MS-SOFC

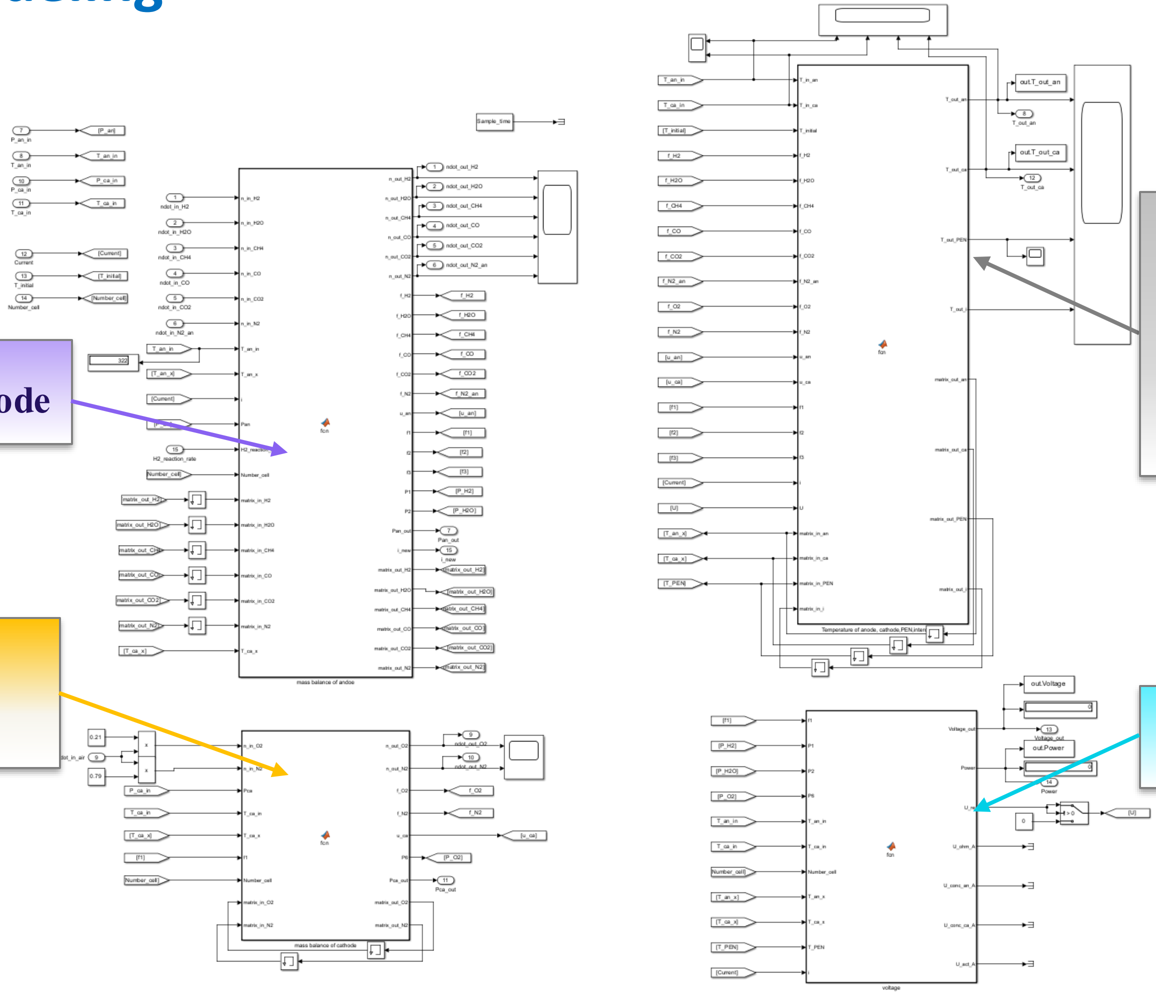

Mass balance of Anode

Mass balance of Cathode

Energy balances
- Anode
- Cathode
- PEN structure
- Interconnect

Electrochemical

MS-SOFC system assembly

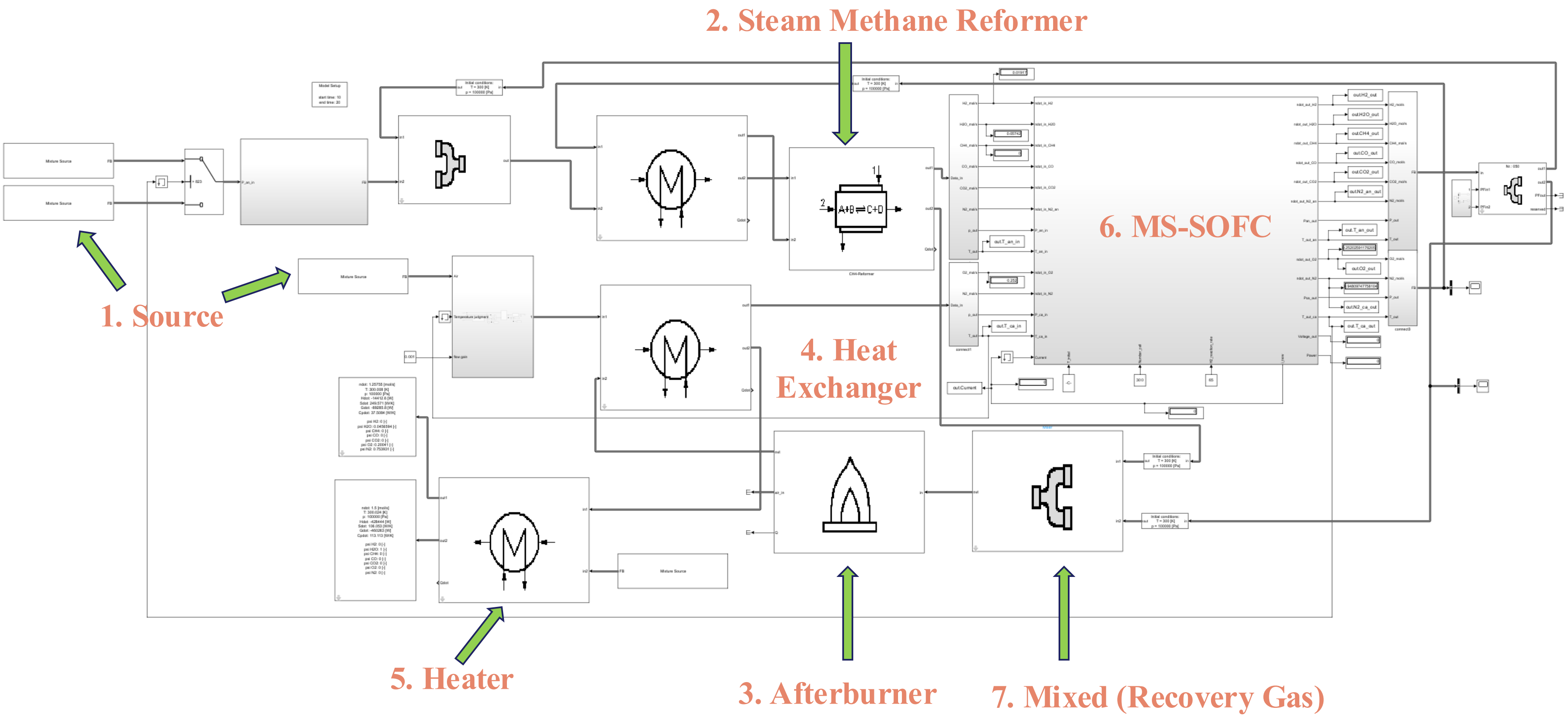

Anode-Supported SOFC (Verification)

Table 1. Structural parameters of AS-SOFC

Structural parameters of AS-SOFC	
Cell length, L	0.4 m
Cell length, W	0.1 m
Fuel channel height, h_a	1 mm
Air channel height, h_f	1mm
Anode thickness, τ_{anode}	500 µm
Cathode thickness, $\tau_{cathode}$	50 µm
Electrolyte thickness, $\tau_{electrolyte}$	200 µm
Interconnect thickness, τ_I	500 µm

Table 2. Operating Conditions of AS-SOFC

Operating Conditions of AS-SOFC	
Pressure of anode, P_{an}	1.3 bar
Pressure of anode, P_{ca}	1.1 bar
Fuel inlet temperature, T_f^0	973 K
Air inlet temperature, T_a^0	973 K
Air feed	21%O2,79% N2
Air ratio, λ_{air}	8.5

Table 3. Physical properties and material parameters of AS-SOFC

Physical properties and material parameters of AS-SOFC	
Anode electrical conductivity, σ_{anode}	$80 \times 10^3\ \Omega^{-1}\mathrm{m}^{-1}$
Cathode electrical conductivity, σ_{ca}	$8.4 \times 10^3\ \Omega^{-1}\mathrm{m}^{-1}$
PEN density, ρ_{PEN}	5900 kg m^{-3}
PEN heat capacity, $c_{p,PEN}$	0.5 kJ $\mathrm{kg}^{-1}\mathrm{K}^{-1}$
PEN thermal conductivity, λ_{PEN}	2×10^{-3} kJ $\mathrm{m}^{-1}\mathrm{s}^{-1}\mathrm{K}^{-1}$
PEN emissivity, ϵ_{PEN}	0.8
Electrolyte ionic conductivity, $\lambda_{electrolyte}$	$33.4 \times 10^3 \exp(-\ 10.3 \times 10^3 / T)\Omega^{-1}\mathrm{m}^{-1}$
Interconnect density, ρ_I	8000 kg m^{-3}
Interconnect heat capacity, $c_{p,I}$	0.5 kJ $\mathrm{kg}^{-1}\mathrm{K}^{-1}$
Interconnect thermal conductivity, λ_I	25×10^{-3} kJ $\mathrm{m}^{-1}\ \mathrm{s}^{-1}\mathrm{K}^{-1}$
Interconnect emissivity, ϵ_I	0.1
Anode diffusion coefficient, $D_{eff,anode}$	$3.66 \times 10^{-5}\ \mathrm{m}^2\ \mathrm{s}^{-1}$
Cathode diffusion coefficient, $D_{eff,cathode}$	$1.37 \times 10^{-5}\ \mathrm{m}^2\ \mathrm{s}^{-1}$

Ref. Aguiar, Patricia, Claire S. Adjiman, and Nigel P. Brandon. "Anode-supported intermediate temperature direct internal reforming solid oxide fuel cell. I: model-based steady-state performance." Journal of power sources 138.1-2 (2004): 120-136.

Mesh validation

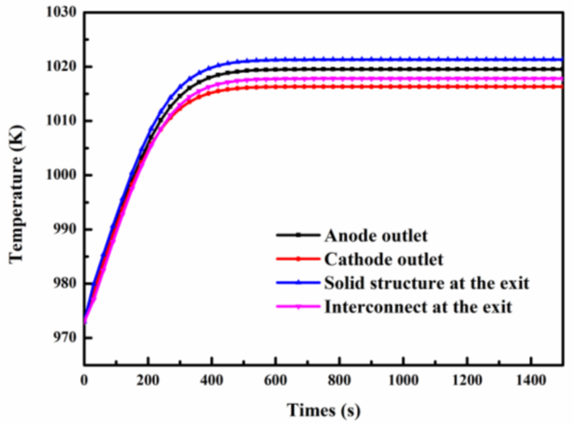

Fig1. The temperature at the outlet of each area at different time points

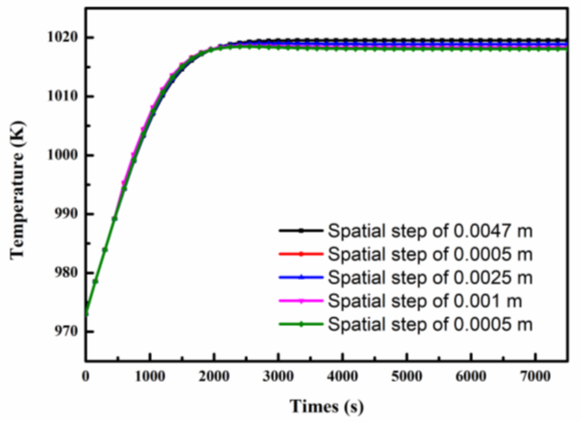

Fig2. Comparison chart of anode outlet temperature results at different spatial steps at different times

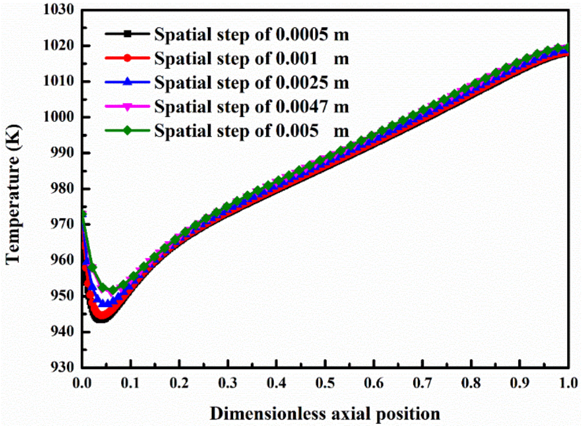

Fig3. Comparison of the Impact of Different Spatial Step Sizes on the Numerical Simulation Results of Temperature Distribution in the Anode Flow Channel

Model validation

Fig.4. Comparison of simulated voltage response with experimental response reported in [23].

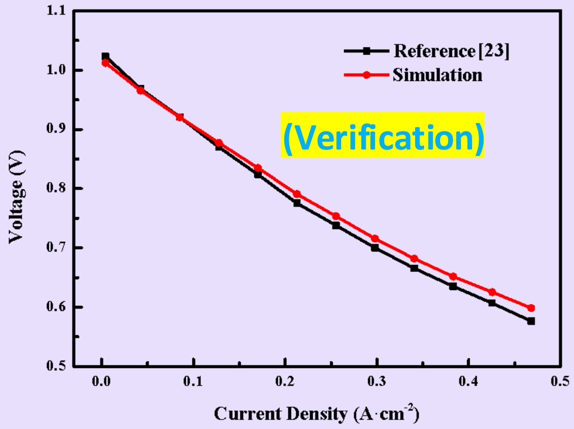

[23] Ref. Aguiar, Patricia, Claire S. Adjiman, and Nigel P. Brandon. "Anode-supported intermediate temperature direct internal reforming solid oxide fuel cell. I: model-based steady-state performance." Journal of power sources 138.1-2 (2004): 120-136.

MS-SOFC

Table6. Operating Conditions of MS-SOFC (Data1)

Operating Conditions of **MS-SOFC (Data1)**	
Pressure of anode, P_{an}	1.3 bar
Pressure of anode, P_{ca}	1.1 bar
Fuel inlet temperature, T_f^0	973 K
Air inlet temperature, T_a^0	973 K
Air feed	21% O_2, 79% N_2
Air flow velocity	3.6 $m\ s^{-1}$
Fuel feed	100% H_2
fuel flow velocity	0.6 $m\ s^{-1}$

Table7. Operating Conditions of MS-SOFC (Data2)

Operating Conditions of **MS-SOFC (Data2)**	
Pressure of anode, P_{an}	1.3 bar
Pressure of anode, P_{ca}	1.1 bar
Fuel inlet temperature, T_f^0	873 K
Air inlet temperature, T_a^0	873 K
Air feed	21% O_2, 79% N_2
Air flow velocity	3.6 $m\ s^{-1}$

Fuel flow rate, gas composition, water-to-carbon ratio, and reforming reaction rate of MS-SOFC.

Pure hydrogen fuel			
0.104 mol s^{-1}	**100% H_2**		
Mixed fuel **0.045 mol s^{-1} H_2, Water to carbon ratio (S/C) H_2O,** **0.015 mol s^{-1} CH_4, 0.007 mol s^{-1} CO, 0.047 mol s^{-1} CO_2**			
	Steam reforming rate		
S/C 2 **(S/C: Water to carbon ratio)**	**50 %**	**75 %**	**100%**
S/C 2.5	**50 %**	**75 %**	**100%**
S/C 3	**50 %**	**75 %**	**100%**

Pure Methane fuel **Water to carbon ratio (S/C) H_2O, 0.026 mol s^{-1} CH_4**				
	Steam reforming rate			
S/C 2	**25%**	**50 %**	**75 %**	**100%**
S/C 2.5	**25%**	**50 %**	**75 %**	**100%**
S/C 3	**25%**	**50 %**	**75 %**	**100%**

Data1. Model validation

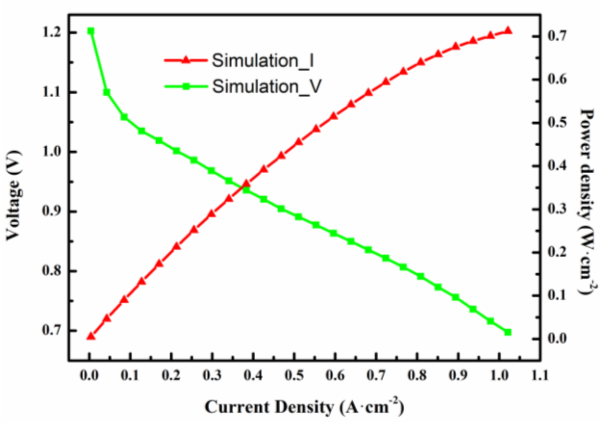

Fig5. Pure hydrogen fuel current density curve

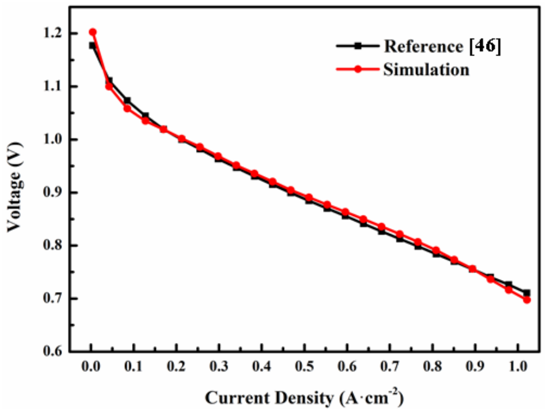

Fig6. Comparison chart of the relationship between voltage, current density and reference value

Data2. Steady state performance analysis

Pure hydrogen fuel, 0.104 $mol\ s^{-1}\ H_2$

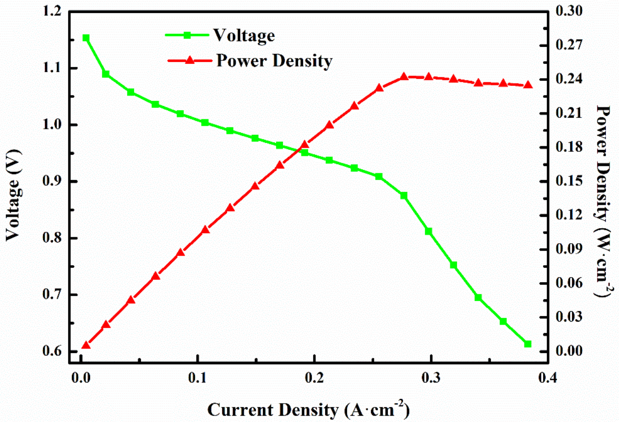

Fig.7. Simulation results for voltage vs. power density characteristics of MS-SOFC with **pure hydrogen fuel**.

(a)

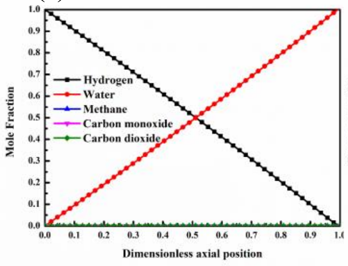

(b)

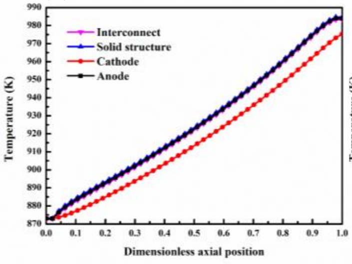

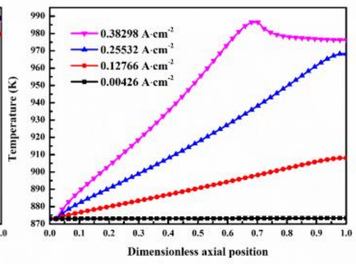

Fig.8. Distribution of hydrogen mole fraction in anode flow channel under peak power density conditions with **pure hydrogen fuel**.

Fig.9. Temperature distribution in anode channel of MS-SOFC with different current densities

Conclusion

The designed model incorporates mass and energy balance equations, as well as electrochemical models. Simulations have been performed to investigate the electrochemical behavior of the MS-SOFC, the temperature distribution within the multi-layer SOFC structure, and the fuel component fractions at the inlet and outlet of the anode channel under the effects of different water-to-carbon ratios (S/C = 2, 2.5, and 3) and methane vapor refining reaction rates (50%, 75%, and 100%). Two fuels have been considered: pure hydrogen and a mixed fuel containing hydrogen, methane, carbon monoxide, and carbon dioxide. The simulations have focused on the problem of maximizing the current density in the MS-SOFC while simultaneously maintaining a low operating temperature of 600°C by controlling the S/C ratio and methane vapor refining reaction rate. **Peak power density (PPD)** under different conditions:

Input conditions	Pure hydrogen fuel	Mixed fuel, S/C=2			Mixed fuel, S/C=2.5			Mixed fuel, S/C=3		
		SMR50%	SMR75%	SMR100%	SMR50%	SMR75%	SMR100%	SMR50%	SMR75%	SMR100%
PPD value	0.24201	0.17889	0.21004	0.23041	0.17422	0.20873	0.22882	0.17271	0.20760	0.22734

Pure methane fuel, S/C=2				Pure methane fuel, S/C=2.5				Pure methane fuel, S/C=3			
SMR25%	SMR50%	SMR75%	SMR100%	SMR25%	SMR50%	SMR75%	SMR100%	SMR25%	SMR50%	SMR75%	SMR100%
0.03255	0.07520	0.12415	0.16381	0.03339	0.07873	0.13018	0.17043	0.03435	0.08007	0.13316	0.17808

- **PPD: Peak Power Density**
- **SMRR: Steam Methane reforming rate**
- **S/C: Water to carbon ratio**

Physical parameters of MS-SOFC fluids

Table 7. Coefficients used to calculate specific heat capacity of MS-SOFC.

	H_2	H_2O	CH_4	CO	CO_2	O_2	N_2
B	2.47906	4.00392	4.00088	3.50055	3.50002	3.50146	3.50031
C	0.95806	0.01059	0.76315	1.02865	2.04452	1.07558	0.13732
D	228.734	268.795	820.659	1550.45	919.306	2235.71	662.738
E	0.45444	0.98763	0.0046	0.00493	-1.06044	1.01334	-0.1466
F	326.843	1141.41	178.41	704.525	865.07	1116.69	680.562
G	1.56039	3.06904	8.74432	0	2.03366	0	0.90066
H	1651.71	2507.37	1.062.82	0	483.553	0	1740.060
I	-1.376	0	-4.469	0	0.014	0	0
J	1671.69	0	1090.53	0	341.109	0	0
M	2.016	18.015	16.043	28.01	44.01	31.999	28.013

The specific heat capacity of MS-SOFC, c_p, is defined using data from ISO 20765-1 [25]. Based on this data, **we derived a novel ideal gas temperature polynomial equation**, referred to as the **Kuo and Liu equation**, to determine the **specific heat capacity (C^0_{pi}) of MS-SOFC**. The coefficients for this equation are provided in Table 7.

$$\frac{C^0_{pi}}{R/M} = B + C\left(\frac{D/T}{\sinh(D/T)}\right)^2 + E\left(\frac{F/T}{\cosh(F/T)}\right)^2 + G\left(\frac{H/T}{\sinh(H/T)}\right)^2 + I\left(\frac{J/T}{\cosh(J/T)}\right)^2$$

Conclusions

- **Four value chains representing opportunities for scaling up Hydrogen in the near term**

1. **To open gateways to lower-cost and lower-carbon hydrogen hubs.**
   - ✓ Europe, United States, Japan, Middle East , Latin America, Taiwan, China, Australia

2. **To Scale up low-carbon hydrogen supply by tapping into dependable demand.**
   - ✓ North America, Europe, Middle East

3. **To reach the appropriate scale for competitive fuel cell vehicles and refueling.**
   - ✓ Japan, Korea, China, Europe, United States

4. **To kick-start international hydrogen trade for the ultimate global low-carbon market.**
   - ✓ Asia Pacific, Middle East, North Africa, Europe

- # Wider Hydrogen Value Chain Risks and Dependencies

- ✓ Blue and green hydrogen competition
- ✓ Markets and regulations, safety and public trust
- ✓ Skills gaps
- ✓ Resource efficiency and embodied carbon in infrastructure
- ✓ The atmospheric greenhouse effect of hydrogen leakages
- ✓ Global production and use of hydrogen and international trade
- ✓ Cost uncertainties of imports
- ✓ Emission uncertainties of hydrogen imports

2025 H2 Energy and Fuel cell Conference

Laboratory Team Members

Thank you for your attention!

Email:
jenn.kun@gmail.com